Nonprofit joint stock company
«ALMATY UNIVERSITY OF POWER ENGINEERING AND TELECOMMUNICATIONS»

Department Information Systems Engineering
Specialty 6M070300 - Information Systems

Admitted to defend
Head of the IS department
Imangaliyev Sh.I.
«____»_____2014 y.

MASTERS DISSERTATION
explanatory note

Title Simulation models of power engineering objects in theory and practice

Master student _____ Sarzhanova A.B.
signature (Full name)

Dissertation supervisor _____ Kazakhbaeva G.U.
signature (Full name)

Reviewer _____ Balgabaeva L.Sh.
signature (Full name)

Almaty, 2014 y.

Nonprofit joint stock company
«ALMATY UNIVERSITY OF POWER ENGINEERING AND TELECOMMUNICATIONS»

Faculty Information Technology
Specialty 6M070300 - Information Systems
Department Information Systems Engineering

TASK
to fulfill the master's dissertation

By master student Sarzhanova Assel Bakhytzhanovna
(surname, name, patronymic)

Dissertation title Simulation models of power engineering objects in theory and practice

Approved by the Academic Council №___ от «___»_____
Deadline for completed dissertation «___»_____
Objective of the research investigation of deformation assessment of power transformer winding based on their frequency characteristics and practical use of FRA method on real object of ЭлектроЮгМонтаж company

List of issues to be developed in the master's dissertation or summary of the master's dissertation:
1. Literature review of existing power transformer winding deformation/displacement diagnostic techniques
2. Analysis of transformer winding faults and type of faults, reasons and causes of failure
3. Determination of influence of winding parameters to the frequency characteristics of the model
4.Development of algorithm to construct equivalent circuit and winding modeling in the Matlab environment
5. Experimental works on different case studies using SimPowerSystems block of Simulink

List of graphical material (with the exact mandatory drawings)
1. FRA simulated plots of power transformer winding
2. Winding model built in the Matlab environement

Recommended main literature
1. И.В. Черных. Моделирование электротехнических устройств в Matlab, SimPowerSystems и Simulink. – М.: ДМК Пресс; Спб.: Питер, 2008. – 288с.

SCHEDULE
master's dissertation preparation

Name of sections, the list of emerging issues	Submission deadlines to supervisor	Remark
1. Representation of Power Transformer in Electrical Power System	02.01.2014 – 02.02.2014	
Operational principles of power transformer	07.01.2014	
Analysis of PT failures and problems	17.01.2014	
Key role of PT in electrical power system of Kazakhstan	22.01.2014	
Transformer winding faults, type of faults	02.02.2014	
2. Modern trends in diagnostic technique of power transformer winding	03.02.2014 – 16.03.2014	
Analysis of existing methods in PT winding diagnostics	12.02.2014	
Literature review of previous efforts done by other researchers	03.03.2014	
Details of FRA method, describe difference between SFRA and IFRA	16.03.2014	
3. Modeling a transformer winding	17.03.2014 – 25.04.2014	
Introduction to Matlab environment. Use of SimPowerSystems block in Simulink	28.03.2014	
Mathematical description of PT model winding	11.04.2014	
Construction of the winding model in Matlab environment	25.04.2014	
4. Experimental works on FRA methods	26.04.2014 – 18.05.2014	
Experimental works with winding model based on space factor	10.05.2014	
FRA simulations for different case studies	18.05.2014	

Date of issuance of the task 20.05.2014

Head of the department _____ (Imangaliyev Sh.I.)
(signature) (Full name)

Dissertation supervisor _____ (Kazakhbaeva G.U.)
(signature) (Full name)

Task fulfillment had taken by
Master student _____ (Sarzhanova A.B.)
(signature) (Full name)

Аңдатпа

Магистерлік диссертацияда трансформатор орам сымының деформациялануын жиілік талдау тәсілімен диагностикалау мәселесінің өзектілігі қарастырылған. Трансформатор орам сымының дефект түрлері мен іс-тәжірибеде қолданыста келе жатқан диагностика тәсілдеріне зерттеу жүргізілген. Имитациялық алдын алу диагностика іс-шарасын жүргізу мақсатында электрқұрылғының құрылымының ерекшеліктеріне сәйкес трансформатор орам сымының түрі, параметрлері таңдалды және талдау жасалды. Бұл жұмыста трансформатор орам сымының жиілік сипаттамасы жете зерттеліп, онымен қоса имитациялық моделі Matlab ортасында эксперименттік жұмыстар үшін жасалынды.

Аннотация

В магистерской диссертации рассматривается актуальность проблемы диагностики деформации обмоток силового трансформатора методом частотного анализа. Описаны дефекты обмоток силовых трансформаторов и изучен опыт проведения диагностики существующими методами. Проведен анализ и выбор типа, параметров обмотки трансформатора с учётом конструктивных особенностей для проведения имитационной профилактической диагностики электрооборудования. В Данной работе проведено исследование частотных характеристик обмоток силового трансформатора, также представлена имитационная модель созданная в середе Matlab с целью проведения экспериментальных работ.

Annotation

In this master’s dissertation current problems in the diagnosis of power transformer winding deformation using frequency response analysis are presented. Defects of power transformer windings, and the experience of the various existing diagnostic methods is described. The analysis are conducted in selecting the type of transformer winding by its parameters based on the design features to simulate damage preventive studies on electrical equipment. This paper presents a study of the frequency characteristics of the windings of the power transformer, also a simulation model built in the Matlab environment is presented to carry out experimental works.

Table of contents

Introduction

Power transformers are among the most expensive and critical units in a power system designed to withstand a variety of stresses and mechanical forces during their service life. Therefore, there is a great interest in its health state. Since power transformers are mainly involved in the energy transmission and distribution, efficiency, quality and economic cost of the Energy Power Supply Companies depends strongly of the transformer reliable service [1]. The mechanical integrity of a transformer winding has a significant impact on the transformer health, which in turn may lead to unplanned power transformer outage. Moreover, power transformer winding maintenance is the time-consuming and cumbersome high cost work, which requires an expert to repair the equipment at the power transformer mounting place or requires transportation of transformer to manufacturer's repair area.

For this reason, to have reliable operation of transformer, it is necessary to identify problems at early stage before a catastrophic occurs. In spite of corrective and predictive maintenance, the preventive maintenance of power transformer must be taken into account to obtain highest reliability of power apparatus like a power transformer.

Nowadays, movement from time-based maintenance programs to condition-based maintenance is a trend in the industry. Instead of doing maintenance at regular, pre-determined intervals, it is carried out if the transformer winding is suspected to be deformed. Hence, there is an increasing need for better non-intrusive diagnostic method to assess the internal condition of power transformers.

Besides traditional methods FRA (Frequency Response Analysis) technique is actively embedded to identify winding geometry of power transformer in the world. The FRA method allows to assess an internal axial and radial deformation of a transformer winding, measurement is done while transformer de-energized and isolated from the power system.

At the current stage of development of FRA-based diagnostics, there are still a few unresolved issues that make it difficult to determine the state of the power transformer windings using this method.

Firstly, it is not possible to determine the type of damage of a power transformer winding using FRA method. To identify the correlation between changes in the characteristics and the degree of development of a power transformer winding defect need a considerable amount of measurements followed by disassembling of power transformer and searching for the winding defect, which is a very time-consuming operation and is not always possible due to lack of technical opportunities to open up the power transformer.

Secondly, the characteristics of power transformer obtained using FRA method are uncomfortable to store and process. Modern computing technology allows to store the results of initial tests in an array of a large number of pixels, but

storage devices expire significantly early before power transformer ages, therefore manufacturers enter the original settings of a transformer into the paper passport.

As a matter of fact, there have been only a few attempts to localize winding deformation and determine extent of deformation along a transformer winding using frequency response data, and hence it is worthy of consideration.

Based on the above mentioned rationale the **purpose of the dissertation work** is clarified as an investigation of deformation assessment of power transformer winding based on their frequency characteristics and practical use of FRA method on real object of ЭлектроЮгМонтаж company. To achieve this purpose it is necessary to solve the following tasks:

- to study the principles of power transformers;
- to analyze and compare the frequency characteristics of the real power transformer windings with and without defects;
- to build PT (Power Transformer) winding model using Matlab/Simulink and investigate its frequency characteristics;
- to explore the transfer function, influence of the parameters to the behavior of the TF;
- to build State space model and investigate the conversion from SS to TF;
- to find correlation between the changes of frequency characteristics of PT winding and the type of winding defect, also between the localization of deformation and its extent;

Scientific novelty of the dissertation work includes:

- proposed a method in deriving transfer function based on the equivalent circuit, by building state space model of the winding;
- introduced an algorithm for synthesizing equivalent circuit based on the measured values of transformer winding and from its FRA results;
- model winding is built using Matlab/Simulink software tool, on which impedance measurements are conducted;
- bode plots are drawn for every case of winding damage and frequency responses are compared on that plots.

Practical significance of the work is determined by the equipment free diagnosis using FRA based on the constructed model of the winding. Implementation of this work in the practice allows to save time consumption in contacting with real transformer winding and to conduct experimental simulations for further investigations and analysis.

Publications on the topic of the dissertation. The main content of the dissertation is described in the article “Method of diagnosis of the transformer winding deformations using frequency response analysis”.

Dissertation consists of introduction, four chapters, conclusion, references and appendices.

In the introduction, actuality, goals and objectives of the dissertation work, obtained results and provisions issued for defense are presented.

Chapter 1 contains information about power transformer operation principles and components, condition of electrical power system of the Republic of Kazakhstan, problems and failures of power transformers, types of faults occurred in transformer winding.

In chapter 2 an overview of the literature devoted to the study of FRA method considered, modern methods devoted to power transformer winding condition controlling is observed, detailed description of the FRA method and measurement principles are presented.

Chapter 3 covers methodologies of obtaining equivalent circuit of the model winding, efficient method of composing transfer function based on that equivalent circuit, also eligibility of the constructed equivalent circuit in localization of damages. Measurements of transformer winding model were taken as a reference data.

Experimental works are fulfilled in chapter 4. The model of transformer winding is constructed using SimPowerSystems block of Simulink and FRA is simulated by producing capacitive changes on winding model. Different case studies are conducted, and FRA results are compared and concluded at the end of the chapter.

1 Representation of power transformers in electrical power system

1.1 Brief description of power transformer and its components

Power transformer is a static electrical device, involving no continuously moving parts, used in electrical power systems to transfer power between circuits through the use of electromagnetic induction. Power systems typically consist of a large number of distribution points, generation locations, and interconnections within the system or with nearby systems, such as neighboring utilities [2]. The complexity of the system leads to a variety transmission and distribution voltages. Power transformers play a key role at each of these points where there is a transition between voltage levels.

The transformer is an electromagnetic conversion device in which electrical energy received by primary winding is first converted into magnetic energy which is reconverted back into a useful electrical energy in other circuits (secondary winding, tertiary winding, etc.). Thus, the primary and secondary windings are not connected electrically, but coupled magnetically. A transformer is termed as either a step-up or step-down transformer depending upon whether the secondary voltage is higher or lower than the primary voltage, respectively. Transformers can be used to either step-up or step-down voltage depending upon the need and application; hence their windings are referred as high-voltage/low-voltage or high-tension/low-tension windings in place of primary/secondary windings [3].

It is known that construction of a power transformer varies throughout the industry. The basic arrangement is essentially the same and slight changes have been done in recent years. High voltage power transformer is a complex device, consisting of a large number of structural components, viz. magnetic circuit (magnetic core), windings, insulation, taps, tank, cooling systems, voltage regulation mechanism, protection and measurement tools.

Magnetic circuit of power transformer contains magnetic flux. Magnetic core is a constructive and mechanical basis of power transformer. It is made from the individual electrical steel sheets isolated from each other. Currently used cold rolled grain oriented (CRGO) silicon steel of grades 3405.3406, allows induction up to 1.7 Tesla. The use of such steel can significantly reduce the cross section of the core due to large allowable magnetic induction, also can reduce the diameter of the winding turns, mass and overall dimensions of transformers. For transformer steel sheets are widely used insulation varnish layer thickness of 0.01 mm. Lacquer film creates a sufficiently reliable isolation between sheets, provides good cooling of the magnetic core, has high heat resistance and is not damaged during assembly.

The rectangular paper-covered copper conductor is the most commonly used conductor for the windings of medium and large power transformers. These conductors can be individual strip conductors, bunched conductors or continuously transposed cable (CTC) conductors. In low voltage side of a distribution transformer, where much fewer turns are involved, the use of copper or aluminum foils may find preference. To enhance the short circuit withstand capability, the

work hardened copper is commonly used instead of soft annealed copper, particularly for higher rating transformers. In the case of a generator transformer having high current rating, the CTC conductor is mostly used which gives better space factor and reduced eddy losses in windings. When the CTC conductor is used in transformers, it is usually of epoxy bonded type to enhance its short circuit strength. Another variety of copper conductor or aluminum conductor is with the thermally upgraded insulating paper, which is suitable for hot-spot temperature of about 110°C. It is possible to meet the special overloading conditions with the help of this insulating paper. Moreover, the aging of winding insulation material will be slowed down comparatively. For better mechanical properties, the epoxy diamond dot paper can be used as an interlayer insulation for a multi-layer winding. High temperature superconductors may find their application in power transformers which are expected to be available commercially within next few years. Their success shall depend on economic viability, ease of manufacture and reliability considerations [3].

Transformer insulation is very important, since reliable operation of power transformer is mainly determined by its insulation reliability. In liquid-immersed transformers oil is the basic insulation in combination with solid dielectrics such as paper, electro-cardboard, hardened paper. In dry-type transformers new types of insulating materials of high thermal stability based on silicone materials are widely used.

The active part of the taps is placed together with the switching devices for controlling voltage in the transformer tank. The main parts of the tank are walls, a bottom and a cover. The cover is used in the installation of bushings, exhaust pipe, mount extender, thermometers and other items. Cooling devices – radiators are strengthened on the walls of the tank. To reduce losses from scattering streams steel tanks are screened from the inside by the packages of electrical steels or by plates made of nonmagnetic materials (copper, aluminum).

Exhaust (safety) pipe on the cover of tank prevents it from tearing during vigorous gas evolution during major damage inside the transformer (short-circuit). The upper end of the exhaust pipe is hermetically closed by the diaphragm of a thin glass or a copper foil. When explosive gas discharge occurs the diaphragm collapses and the pressure in the tank decreases, which prevents it from deforming. The upper chamber of the exhaust pipe and the air space above the oil in the expander are connected by a tube. It is necessary to equalize the pressure on both sides of the diaphragm when the volume of oil changes in the normal operating conditions. Currently, instead of exhaust pipes mechanical spring safety valves are applied, which are mounted on the upper portion of the wall of the power transformer. The valve is activated when the pressure in the tank is increased up to 80 kPa, and is closed when the pressure is below 35 kPa.

The common elements of power transformer discussed above are represented in Figure 1.1, where as an example of power transformer, liquid-immersed power transformer is chosen [4].

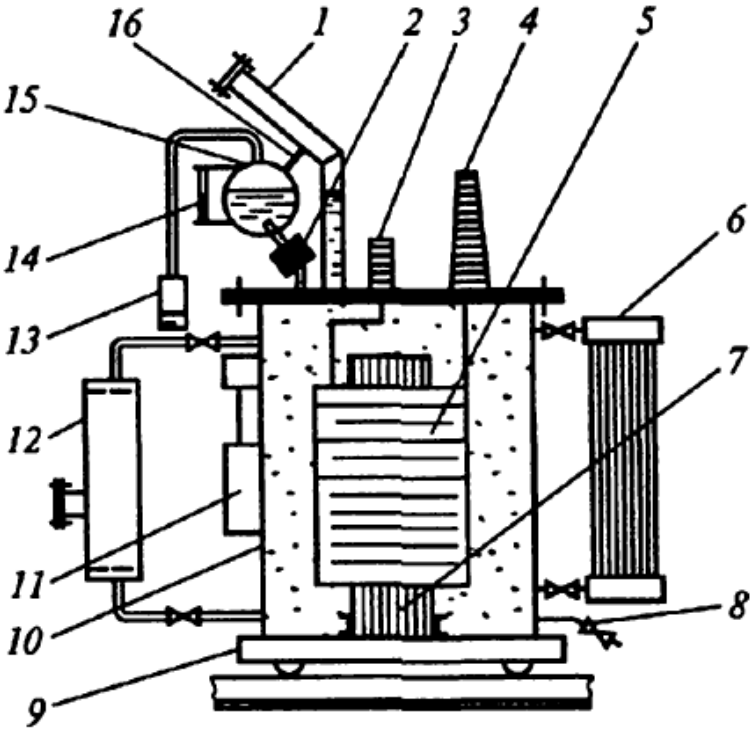

1 – exhaust pipe, 2 – Buchholz relay, 3 – HV input, 4 – LV input, 5 – HV/LV windings, 6 – cooling system radiators, 7 – magnetic core, 8 – oil drain tap, 9 – roller trolley, 10 – tank, 11 – load control device (LCD), 12 – thermosyphon filter, 13 – air drier, 14 – oil-level indicator, 15 – extender, 16 – connecting tube.

Figure 1.1 – Structural layout of liquid-immersed power transformer:

1.1.1 Basic specifications of power transformers.

Diverse use of power transformers caused the necessity of building them in wide range. Power transformers characterized by their nominal power, voltage class, condition and operation, constructive execution. According to the nominal power and voltage class power transformers are divided into several groups based on their overall dimensions as shown in Table 1.1.

Table 1.1 – Nomenclature of power transformers

No. of overall dimension	Power range in kVA	Voltage class in kV
I	Up to 100	Up to 35
II	100 to 1000	Up to 35
III	1000 to 6300	Up to 35
IV	Over 6300	Up to 35
V	Up to 32 000	35 to 110
VI	32 000 to 80 000	Up to 330
VII	80 000 to 200 000	Up to 330

Table 1.1 continued

VIII	Over 200 000	Up to 330
	Irrespective of power	Over 330
	Irrespective of power for DC power line	Irrespective of voltage

Depending on the operating conditions, load classification and operating mode power transformers classified as general-purpose transformers, regulation transformers, transformers of special purpose (mine, tractive, transformative, inrush and etc.).

Transformers are manufactured as three-phase or single phase, two winding or three winding transformers. Three phase transformer is mostly preferred due to economic benefits over a single phase transformer having the same reliable operation. Single phase power transformers are used only at the highest powers at voltages over 500 kV with the aim of decreasing transport mass.

Autotransformer is the type of multi-winding transformer. Two windings of autotransformer are connected electrically. Three winding autotransformers of three phase or group of single phase are widely used in electrical power system. These transformers are preferable instead of conventional transformers due to economic gain to connect effectively grounded networks with the voltage of 110 kV and over with respect to the nominal voltages not exceeding 3 - 4. However, autotransformers are unsuitable to connect ungrounded networks.

Subject to cooling systems transformers are divided into dry-type transformers, liquid-immersed transformers and transformers with non-combustible liquid dielectric.

1.2 Electric power system of the Republic of Kazakhstan

Electric power system (EPS) of the Republic of Kazakhstan operates in parallel with EPS of the Russian Federation and EPS of Central Asia. The power system of Kazakhstan due to its geographical location is divided into three zones – North, South and West.

According to the condition of power system stated in January of 2009, electricity production in Kazakhstan is carried out by 60 power plants with total installed capacity of 18,992.7 MW. However, the available capacity is 14,558 MW, which is 23.3% less than the installed capacity and the actual operating power - only about 12,500 MW. To date, the possibility of annual generation of electricity in Kazakhstan with the existing generating capacity, according to official data, is not more than 82 - 84 billion kWh of electricity without power reserves.

In recent years there has been a steady increase in demand for electricity. In some regions, such growth has led to a shortage of capacity in terms of the peak consumption in winter. The growth rate of electricity consumption in the south and west of Kazakhstan are even higher (up to 12 - 14%) than the average for the country. For example, in the network of JSC "AZhK" (ОАО «АЖК») increase in

power consumption has taken place since the first years of reconstruction after USSR fall, and at the beginning of 2009 it raised up to 20% than the maximum consumption in 1990. The second circuit line “North-South” has been rendered to reduce the shortage, however the electricity problem in the south part is still unresolved.

Currently there is a positive trend of decreasing difference between consumption and electricity generation. Electricity production and consumption for the past years are represented in Table 1.2 [5].

Table 1.2 - Analysis of production and consumption of electricity in the Republic of Kazakhstan (in billions of kWh)

Index	Years											
	1990	2000	2001	2002	2003	2004	2005	2006	2007	2008	2009	2015 prediction
Production	83.0	51.4	55.4	58.3	63.9	66.9	67.8	71.7	76.4	80.0	78.4	103.45
Consumption	100.4	54.4	57.4	58.7	62.4	64.8	68.4	71.9	76.4	80.6	77.9	100.5

The Government of the Republic of Kazakhstan has taken complex actions, and systems of maximum tariffs to cover the existing loads and to improve the reliability of electricity supply the power of 1073.5 MW was additionally added in 2012. Namely:

- the block No.8 with the power of 500MW is entered In Pavlodar region at GRES-1;

- Moinak hydroelectric station (Мойнакская ГЭС) put into operation with the total capacity of 300 MW in Almaty region.

In 2012, Kazakhstan produced 90.2 billion kW · h of electricity, 4.7% more compared to 2011. Electricity consumption in 2012 amounted to 91.444 billion kW · h, compared to the year 2011 more than 3.8%. These data proves the lack of electricity, in spite of significant increase in electricity production in 2012.

Lack of energy can be a significant deterrent to the development of industry and economic growth. This is a stumbling block on the path to sustainable development of Kazakhstan, as electricity is an inertial sphere in the sense that to enter new capacity a fairly long time is required for intensive implementation.

1.2.1 Power transformer failure and problems

Resource park of electrical equipment installed in existing power plants, substations in electrical networks and industries is out of its service life and needs in replacement or upgrade. Therefore, a global replacement and modernization of a significant proportion of the electrical equipment is intended. The presence of significant deterioration of generating equipment limits the power generation by the current plants.

According to the Ministry of Energy and Mineral Resources, on 01.01.2009, depreciation of equipment in the energy sector of the republic represented as:

- generating equipment - 70% ;
- electrical networks - 65% ;
- heating networks - 80%.

According to the press service of JSC “AZhK” percentage of equipment wear in Almaty and Almaty region is in the range of 70-90%. The approximate amount of investment by the developed investment program for the period 2009-2011 is 68 billion tenge. The situation in other regions is not better.

A significant part of the energy is lost in the power transformers of the power system. According to the data given in 1975, energy loss in power transformers amounted to 7% of all electricity generated in the country (USSR) or 70 billion kWh. The share of power losses in the transformer tends to increase due to increased ratio of power transformers to power generators. Especially great losses are observed in 6-10 kV transformer networks which represent 67% of the total losses in these networks; lost in 35-110 kV transformers more than 45% of network losses; considerable energy losses occur in the step-up transformers. Obviously, the problems of reducing energy losses in power transformers are relevant.

It is known that energy loss in power transformers are made up of the energy loss of idling (losses in the magnetic circuit) and short-circuit energy loss (loss in the windings). The transformer loss is the energy losses which arise in a magnetic circuit, that is, in the steel of the transformer and the electrical losses which arise in the windings of the transformer. Mechanical losses are impossible in the power transformer, because it has no moving parts. Consequently, the electrical energy cannot be converted into mechanical energy.

On the basis of the above information it can be said that magnetic core and windings of power transformer play key roles in the power transformer. Failure or damage found on that elements can lead to the transformer failure. Main types of transformer faults regarding magnetic core and transformer winding are shown in Table 1.3.

Table 1.3 – The main types of transformer damages

Main fault types	Signs of damage
Magnetic core	
Defects between the insulation sheet	Deterioration of oil (decrease flashpoint, hyperacidity). Increased load loss
Local closure of steel plates and “fire” in steel	The appearance of the gas in the gas relay and operation of gas protection to the signal. Decrease in flashpoint of oil. Specific sharp smell and dark color of the oil due to its decomposition (cracking). Increased losses and no-load current.
Increased vibration of magnetic core	Abnormal buzzing, rattling and buzzing in a laminated magnetic circuit. Invalid buzz at the butt of the magnetic circuit.
Grounding break	Crackling inside the transformer at a higher voltage
Increased gaps in the joints between the plates of the active part. Overestimated the thickness of gaskets in the joints of the yokes and columns in the butt magnetic core	Increased load current losses under normal idling
Winding	
Coiled circuit	Operation of gas protection to turn off (gas - flammable, white-gray or bluish color). Abnormal heat, sometimes with a characteristic gurgling oil. The slight increase in primary current. Different resistance of the individual phases to DC. Operation of differential and overcurrent protection, if it is already installed on the primary winding (with the significant damage)
Interruption in the windings	Operation of shielding gas due to the arc generated in a cliff and decomposing oil
Break on the body	Operation of gas, overcurrent and differential protection. Release of oil through the protective pipe
Interphase short-circuit winding	Operation of gas, overcurrent and differential protection. Release of oil through the protective pipe (circuiting tapping and circuiting on inputs)
The closure of parallel wires of in the turns of continuous winding, close to its beginning or end	Increased load losses at normal idling current
Closure of parallel wires in the helical winding coils in the place of transposition	Increase in short-circuit loss
Parallel connection of coils with unequal number of turns	Overheating of windings from circuiting currents
Breakage of one or more wires in parallel windings	Increase in short-circuit loss, also in short-circuit voltage

Generally, transformer failures can be defined as follows [6, 7]:

- any forced outage due to transformer damage in service (e.g. winding damage, tap-changer failure);

- any problem that requires removal of the transformer to a repair facility, or which requires extensive field repair (high moisture levels, excessive gas production).

The normal operation of a power transformer is an outcome of several subsystems, such as, electrical, mechanical, thermal, insulation, etc. Therefore transformer failures can be categorized as electrical, mechanical and thermal. The cause of failure can be internal or external. Table 1.4 shows typical causes of transformer failure.

Table 1.4 – Internal and external causes of failure

Internal	External
Insulation deterioration	System overload
Internal winding resonance	System faults (short circuit)
Oxygen	System switching operations
Overheating	Lightning strikes
Partial Discharge	
Loss of winding clamping	
Moisture	
Solid contamination in the insulating oil	
Design and manufacturer defects	

The investigation of transformer problems or failures is in many respects similar to medical procedures.

1.3 Mechanical integrity of a transformer winding

Winding deformation of transformer may be due to the mechanical and electrical faults. Mechanical faults occur in the form of displaced winding, hoop buckling, winding movement, deformations and damaged winding. They may be due to the loss of pressure, vibration during transportation and also excessive mechanical force during a close-up short circuit fault. Winding movements may also result from stresses induced by electrical faults such as an interturn's short circuit as a result of lightning strikes. It may also result in insulation damage.

The deformation can also be due to ageing of paper. As a transformer ages the insulation shrink and the clamping pressure may be lost which reduces its voltage withstand strength. During normal operating conditions the transformer winding suffers from internal axial and radial forces due to the flow of current in the windings. The transient condition challenges mechanical integrity of the winding significantly. Winding deformations in transformers are difficult to establish by conventional methods of diagnostic tests like ratio, impedance/ inductance,

magnetizing current etc. Deformation results in relative changes to the internal inductance and capacitance of the winding. These changes can be detected externally by low voltage impulse method or FRA method.

1.5 Necessity of deformation investigation of transformer winding in practice

The main subject of this dissertation research is the investigation of radial and axial deformations of the winding by determining the causes of fault and solutions to prevent the failure. Due to the intensive growth of computational technology there is a need in development of diagnostic techniques to get exact values of measurement and accurately assess the condition of the electrical equipment.

There are a few companies working in the sphere of electrical equipment condition monitoring, diagnostics and assessment in Kazakhstan. Some of them are JSC Scientific-Industrial Center "Eleteh" (АО НПЦ «Элетех»), LLP "ElektroUgMontazh" (ТОО «ЭлектроЮгМонтаж»), LLP "Technosila-Kazakhstan" (ТОО «Техносила-Казахстан»), JSC "KazRemEnergo" (АО «КазРемЭнерго»), diagnostics and maintenance center "TechEnergo" («ТехЭнерго») and etc.

Basically this research has been conducted with the support of LLP "ElektroUgMontazh", where study of winding deformation diagnostics is highly appreciated.

The LLP "ElektoUgMontazh" is one of the leading companies in the electrical power system of Kazakhstan. Company is well-known by its transportation skills of heavyweight and oversized loads in Kazakhstan and CIS (Commonwealth of Independent States). Mainly company is targeted in transporting high voltage power transformers, mounting of the transformer in the power station, and in carrying maintenance works on power transformers.

So far company was successful in transporting, mounting and diagnosing the condition of power transformer in following works carried by them [8]:

- transportation of autotransformer АТДЦТН -125000/220/110/10 kV with the weight of 120 tones, work provided by JSC "Kazremenergo" (АО «Казремэнерго»);
- maintenance of reactor РОДЦ – 60000/500, provided by JSC "KEGOC";
- demounting, mounting and transportation of autotransformer АТДЦТН - 125000/220/110/10 kV, provided by LLP "EnergoPromStroiService" (ТОО «ЭнергоПромСтройСервис»);
- replacement of autotransformer 250MWA with the voltage of 220/110/10 kV, provided by JSC "KEGOC" in Karaganda and etc.

Mounting of transformer in the power plants is accurately carried, and primary measurements of transformer winding are fixed for further investigation of transformer winding condition. Company provided with the primary measurements

of some windings of actual transformers, also for the purpose of research intentionally have built winding model.

Since power transformer is high cost electrical equipment and the measurements of winding are often taken by disconnecting it from power grid, which is not desirable and mostly not allowable due to its impact to power system, model winding becomes as a solution.

2 Modern trends in diagnostic techniques of power transformer winding

Currently, all used transformer winding condition control methods are based on the comparative data analysis of primary and current measurements. Data obtained from measurement during acceptance test and introduced in the transformer passport or the measurements obtained in the first use of that method referred as a primary data.

The occurrence of defects and damage in some cases causes change in active and inductive winding resistances, and current and load losses, thus changes occurred in electromagnetic parameters of transformer may indicate a defect of winding. Methods of measuring DC winding resistance, measurement of current and no-load losses, fault resistance, as well as the transformation ratio are based on controlling of winding parameter values.

2.1 Description of control methods of transformer winding geometry

Existing control methods of transformer winding geometry are listed below:

a) Method of measuring DC winding resistance. The measurement results are compared with primary data, or between phases. The measurement results are considered as satisfactory if the values not more than 2% of deviation [15].

If there is a significant amount of short-circuited turns then measured DC resistance of windings, typically smaller, while breakage or inappropriate contact connections exceeds the value in the data sheet or the protocols of the previous measurements.

The sequence disruption of change in DC resistance of power transformer winding taps is a sign that taps on the switch connected wrongly. Thus the deviation of one of the measurements from the previous measurements and factory data indicate a defect in winding connection with the switch or tap violations within the winding;

b) Method of measuring current and no-load losses. Losses and no-load current at rated voltage are important characteristics for manufacturing quality control, as well as transformer maintenance requiring lamination of top yoke of the magnetic core. For three-phase transformers loss value should not differ from passport (primary data) by more than 5%. For single-phase transformers difference in the values obtained from the original should not be more than 10%.

However, the gradient increase in loss during measurement at the reduced voltage after several years of operation, is often observed in a defect-free equipment. In assessing the no-load current changes should bear in mind that in most cases the defective condition is characterized by the difference between the values of the currents in last phases or as compared to the previous measurements of more than 10% [15];

c) Definition of transformation coefficient. The measurement results are compared with the calculated or passport data. The measurement results are considered as satisfactory if the values not more than 2% of deviation [15]. It is

evident that during operation the transformation ratio can be changed only as a result of damage, and the tolerance is determined mainly by the measurement error. In cases where the voltage control stage less than 2%, and to check the quality of repair with replacement of winding, such precision measurements may be insufficient. IEEE standard defines tolerance no more than ± 0,5%.

The above methods can detect serious damage windings such as coiled or open circuit, while determination of the presented deformation or weakening of the compacts using a method of DC resistance measurement of winding, measurement of current and no-load losses, or method of transformation ratio are impossible;

d) Method of measuring fault resistance Zk. Widely used due to operational circular number С-02-88 (№ Ц-02-88) [2, 3], the measurement by this method is carried out in accordance with [15]. Condition assessment of the transformer windings are produced by comparing the measured resistance values by phases with the previous measurement, and between the phases. Value of the relative change in the event of Zk is dependent on the design of the winding of the transformer. Usually maximum deviation normalized to the level of 3%. This method has low sensitivity to certain types of deformations, namely, to deformations which do not alter the volume of the main channel (channel scattering);

e) Method of frequency response analysis. According to the conclusions of the working group CIGRE WG A2.26, based on a generalization of international experience, the method of frequency analysis (FRA - Frequency Response Analysis) is determined as the most sensitive method for diagnosing mechanical state of the transformer windings. FRA is a developed method of LVI proposed in the 60s by Lech and Tyminsky [10] and received widespread in the world for the diagnosis of PT winding deformations due to the impact of short-circuit currents.

The essence of the FRA is as follows: from a special generator to the input of the winding (or neutral) probe signal is applied (pulse or sinusoidal) and from the input of other windings reaction response of the winding from the impact of the probing signal is represented in oscillograms. Recorded oscillograms are analyzed in the frequency domain, for example by rapid Fourier transform. The spectrum of the input and output signals obtained using FRA method is used as an initial data for calculating transfer function (TF), even though in some cases oscillograms are used as well as spectrum in the analysis of winding condition.

The method is based on the principle of successive measurements. Criteria for defect detection in power transformer is the degree of difference between the primary and current measurement. To determine the integral gain r correlation is calculated that varies from 0 to 1. Thus if kr> 0.98, it is considered that the change in the condition of the windings have happened, if 0.96> kr> 0.98 is considered that in the windings of minor changes have occurred, kr if <0.96 is considered that in the winding may be significant changes. The disadvantage of this approach is that, despite the change in the frequency characteristic resonances winding value kr can enter into a valid interval, which would for a false conclusion of a satisfactory condition of PT.

The measurements obtained from new transformer right after its installation or the measurements got after full maintenance of transformer are represented as primary measurement data. Results of the initial survey conducted by the frequency analysis, called normogram and the rest following survey results referred as defectogram.

Any change in the geometry of the windings due to deformations, displacement, dispressing leads to the respective change in the parameters of the winding, viz. capacitance, inductance and resistance, hence change in the reaction of winding to the probe signal is observable. Character of change of the frequency spectrum of the response depends on the characteristics of deformations.

FRA today strengthens its position as a reliable means for controlling the winding of power transformer allowing not only to identify a defect in the early stages of its development, but also to evaluate the state after installation of the transformer to the workplace or leakage fault currents. At the current stage of development of the FRA frequency ranges are defined to corresponding of same or different active components of the power transformer portion. For example, magnetic core has an influence on the frequency characteristics of power transformer in the range of 10 – 1000 Hz, influence of connected wires between the winding and coil correspond to the range of 1 – 10 kHz, influence of winding itself is in the range of 10 – 1000 kHz. However, given the above-mentioned disadvantages, we should recognize that the FRA requires the further development and deeper study.

There is a tendency for the joint use of the experience of short circuit and the FRA, which increases the reliability of the results. Thus fault resistance is produced even on power transformers below 125 MVA which is not required under § 6.12 [9]. The measurement results of FRA are complementary to the results of short circuit experience.

Widespread use of FRA prevents insufficient elaboration of the method, difficulty in measuring results of certification, and complexity of their interpretation. However, a perspective method is recognized and actively implemented in the leading energy companies of the U.S., UK, China, Russia and Kazakhstan.

FRA method can be implemented using two approaches: pulse and frequency.

In the impulse approach (IFRA - Impulse Frequency Response Analysis) low-voltage pulse (standard, double exponential, rectangular) generator is used as a source of probing signal; dual-channel ADC simultaneously records two signals: channel 1 – rectangular sounding pulse input, channel 2 - impulse current transition – reaction coil attached to the impulse. Further, depending on the chosen algorithm of analysis for the recorded input signal x(t) and the response y(t) calculation of their spectral densities is performed, which are the initial data for calculating TF.

In the frequency domain approach (SFRA - Sweep Frequency Response Analysis) sine wave voltage generator is used as source probing signals varying over a wide frequency range - from several hertz to several megahertz. Dual

channel of ADC through the 1st channel records signal applied to the winding input, through the 2nd channel records winding reaction to the applied exposure. Further, the TF is calculated similarly as the ratio of input and output signal spectrums.

The resultant measurement of changing characteristics using oscillograms, spectrum and transfer function (TF) have a number of advantages and disadvantages. Oscillograms, that is, usually used for quality control of the transition process caused by the test signal, and cannot provide information about changes in the resonance frequencies. The advantage of the spectra is its informativeness in the entire measurement range, however, their shape dependent on the shape and amplitude of the spectrum sounding impulse, which imposes limitations in comparing the spectra of various PT and also in conditions of identity of sounding impulse parameters (shape, amplitude, duration) for all measurements.

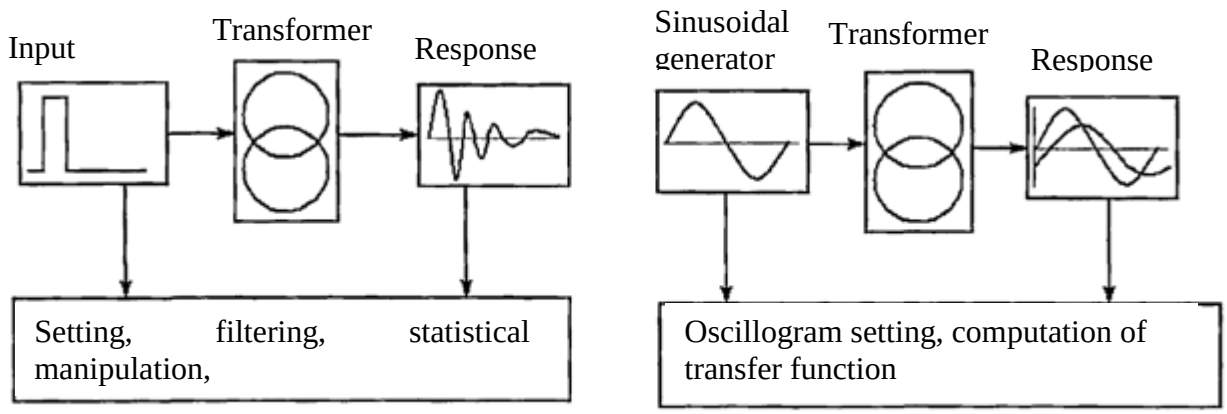

a) b)

a) impulse approach, b) frequency approach

Figure 2.1 – Schematic diagram of FRA measurement

Transfer function is the most visible feature to issue a report of status on surveyed power transformer as it is independent on the shape and amplitude sounding impulse spectrum. Nevertheless, the application of TF in impulse approach has limitations in the frequency range, because the frequencies, where the amplitude spectrum approaches zero, the value of TF may increase sharply.

This is because TF is calculated by the formula shown below:

$$k(f) = \frac{A_{out}(f)}{A_{in}(f)}, \tag{2.1}$$

where $k(f)$ – transfer function;

$A_{out}(f)$ – amplitude of output signal;

$A_{in}(f)$ – amplitude of input signal.

Amplitude spectrum of sounding impulse is in the denominator, so when $A_{in}(f) \to 0$, $k(f) \to \infty$. In practice, it leads to an increase of error in calculation

of $k(f)$ at frequencies mentioned above and lower informativeness of that type of curve, with respect to state analysis of the winding. Therefore, in the case of impulse approach TF curves should be compared with the curves of sounding impulse spectrum and most informative frequency bands should be selected in order to avoid false determination of TF changes.

The high sensitivity of the method due to the fact that even minor local changes in the position of elements windings (coils, taps) lead to a sharp change of corresponding capacities and induction, respectively, to the change of the natural oscillation frequencies of the winding. Different types of deformations lead to changes in different bands spectrum.

Results of measurement conducted for the same object by same measuring schemes using frequency approach significantly coincides with the results of measurement conducted using impulse approach. Concurrently, frequency approach has such lack as much more time is spent in the measurement compared to the impulse approach.

2.2 Literature review of research on winding deformation diagnostic methods

2.2.1 Research directions in the field of winding deformation diagnostics

The first mention of LVI method found in the article of the Polish scientists, electricians Lech and Tyminsky [10]. In the 80s of the last century, LVI method started its development and widely spread over the world. Publications dedicated to the control methods of power transformer winding condition found in both foreign and domestic periodical literatures as well as in textbooks. With the development of computer technology it became possible to switch from consideration of the characteristics of power transformer in the time-domain to analyze them in more a visible frequency-domain, so the LVI method further developed in a form of FRA method. In perspective, previous efforts in the field of transformer winding geometry diagnostics can be classified into the following:

a) Detecting deformation in transformer winding. Ability of monitoring methods to detect the smallest change after introducing a physical deformation (i.e. axial, radial, etc.) on actual transformer windings (either specially manufactured for this purpose or foraged from discarded units) was examined [4,7,8]. The task of distinguishing the type-of-fault based on changes observable in the transfer function spectrum has been reported [13]. It is shown that radial and axial winding faults produce changes in transfer function at different frequency intervals, thereby providing a discriminating feature. In [9], a correlation is shown to exist between a particular mechanical deformation in the winding and changes affecting only particular type of circuit elements of the ladder network. Another goal pursued has been to determine the smallest deformation, which could be unambiguously detected. In [13] it was reported that as low as 10mm of axial displacement could be detected. Notwithstanding these progresses, interpretation of monitored data has

largely remained subjective, i.e. based on visual comparison or a matter of expert opinion;

b) Correlation between type-of-fault and measured quantity. Frequency response of the transformer winding is sensitive to its physical parameters. Hence, the resonant pole frequencies, phase and amplitude of the impedance function will show changes with winding condition. In [14], Ryder concludes that different types of faults dominate the frequency response at different ranges, viz. low frequency response is affected by ungrounded core and short-circuited turns, the medium frequency response is sensitive to faults due to both axial and radial deformation and high frequency response is largely contributed by localized winding damage. The type-of-fault is correlated with parameter changes in [15], viz. inductance for disc deformation, shunt capacitance for radial deformation, series capacitance for insulation ageing, etc. However, a general consensus has not emerged on what type-of-fault is responsible for which parameter change and their frequency ranges;

c) Development of circuit models. Another topic of interest has been to either build circuits (mostly non-ladder networks), starting from data available from terminal measurements and experimental tests performed on actual transformers. Further developing lumped-parameter models from the design data and subsequently validating them against terminal measurements have been attempted. Such models fail to match the terminal characteristic in the high frequency range. The underlying idea is to construct networks corresponding to fault-free and faulty cases. A comparison amongst them would show the existence of a fault and also reveal correlations, if any; between the fault and the circuit element that has undergone a change. Although, these circuits accurately represent the terminal characteristics, their utility is limited since these circuits (most of them) are not physically realizable (resistance estimated is negative, inductance is far too high to be practical, etc.). Being non-ladder networks, it is difficult to visualize how they could be useful for fault localization;

d) Rational function approximation. Estimation of a rational function approximation (in s-domain) to accurately describe the measured terminal characteristic has also been investigated. These functional approximations result in compact models of the transformer and these have been found useful to accurately represent the time/frequency domain behavior of transformers, especially in power systems study;

e) Localization of faults in a model winding. In a recent contribution [12], it was shown how a ladder network equivalent circuit (with all mutual couplings) could be synthesized, starting from measured driving-point frequency data and adopting an iterative circuit synthesis approach. In this, physical length of a model coil was mapped to discrete nodes in the equivalent circuit, thereby rendering fault localization a possibility. Fault localization was achieved to a limited extent, i.e. for capacitance changes alone.

Therefore, from the above description, it is obvious that there are still unresolved issues in any research efforts (regarding winding

displacement/deformation) in actual transformer windings. Hence, it is needless to mention the significance of solving that problems.

2.2.2 Literature review of previous efforts

The following are major publications related to the development of FRA and modeling of power transformer winding.

In [16] the experimental studies of FRA performed using diagnostic equipment “Impulse-7M”. Surveys were conducted on TM-1000/10 transformer by purposely introducing damage to the regulating section of HV winding and by measuring circuit. Some results of the surveys were presented in the work. Electrical circuits having the greatest sensitivity to this type of damage were revealed. Based on the survey results following terms were concluded:

- FRA has higher sensitivity compared to the method of measuring fault resistance Zk;
- increase in reliability of the FRA measurement results with applying different defectogram schemes.

In [17] so-called sweep-frequency generator and frequency analyzer is applied. Varying frequency sinusoidal signal with the amplitude of 2 V is applied at the beginning of the winding. To the beginning of the winding through shielded coaxial cables input of frequency analyzer is attached. The other end of winding (e.g., neutral) is connected through a current transformer to a second input of the analyzer, wherein the windings which are not involved in the measurements are grounded. Feedbacks of the winding are determined by frequency-dependent impedance and (or) full conductivity of each winding and estimated by amplitude and phase for two standard frequency bands: 50 Hz - 500 kHz and 200 kHz - 2 MHz. Each feedback of the windings is analyzed by determining changes in resonance (normogram is required) by determining the difference between the responses of the three phases of the transformer, by determining differences between the responses of a transformer of similar construction. The article gives a few examples.

In [18] an attempt is made to determine the fault location on the model 250 MVA transformer with a rated voltage of HV winding equal to 525 kV. No description of the measurement procedure is provided. Windings are not participating in the trials are short-circuited. The spectrum for simplified equivalent circuit of the windings (of 12 elements and 5 nodes) is calculated, imitations of HV winding damage (shorted several sections at the bottom of the coil) and the breakup of the winding are produced. Frequency range - up to 1 MHz is considered. The results showed good agreement between the calculated and actual changes in the spectrum associated with the damage; concluded that the change of pressing only leads to a change in the amplitude peaks of the generated transfer function, but does not change its frequency.

In [19] lots of measurement have been by LVI method on the transformers of the same type, at least one of the transformers had significant deformation in the LV winding. These deformations have shown a correlation in characteristics of two frequency regions of the spectrum. These features (symptoms, differences) are very small and can be easily missed or recognized as acceptable based on the results of measurements of other similar transformers. Physical damage can also be easily missed at the most superficial examination of the visible parts of the windings. Conclusions on the drawings:

- measurement results obtained using frequency response analysis method in the range of over 2 MHz are unreliable;
- transformer with or without oil has spectrum with shifted frequencies (without oil - increased frequency).

In [20] very efficient methods have been described for the computation of the turn-to-turn parameters of transformers. The leakage inductances are obtained in a simple way and with reasonable accuracy by an approach based on images, analogous to the methods used in the calculation of transmission line parameters. The validity of the method has been confirmed by comparison with short circuit inductances computed with the method of finite elements and a classical design formula. The capacitances are obtained very accurately by a charge simulation approach.

The turn-to-turn parameters are intended to be used in a reduced order winding model, in conjunction with the iron core magnetization model, for the complete modeling of transformers for calculation of transients.

In [21] off-line and on-line monitoring of power transformer in service is demonstrated.

The characteristics of off-line monitoring arc demonstrated by on-site measurements performed in a 220 kV substation (Figure 2.3). Power transformer T1 (200 MVA, 245 kV/110 kV/10.5 kV) was switched on the h.v side by an SF_6 circuit-breaker (S1). On the l.v. side the transformer was connected to a regulating transformer (T2) by a cable (L2). The circuit breaker S2 on the l.v. side of the regulating transformer was always switched off during the measurements. The voltages at the three h.v. terminals were measured in the frequency range from 25 Hz to approximately 2 MHz using the measuring taps of the bushings. As a system response of the transformer the neutral current to ground was measured with a Rogowski coil in the frequency range from about 30 kHz to 2 MHz. The signals were recorded by a digitizer working with a sampling frequency of 10 MHz and a resolution of 10 Bit.

2.3 FRA measurements performed in the industry

At the current stage of FRA development, there is no classification of frequency characteristics of various types of power transformer winding. The main factors affecting the form of the frequency characteristic of PT winding:

- the design of the PT winding;
- manufacturer;
- the history of PT exploitation.

Influence of factory on the form of frequency characteristics is shown in the diversity of technologies in manufacturing PT windings, use of different insulating and conductive materials, choice of key sizes of PT, ratio of the average length of the channel between the windings to the height of the coil which in the literature referred as β. For example, insufficient quality leads to the short circuit of winding coil and premature failure of power transformer.

Measurements on frequency characteristics of power transformer winding are conducted in the "ElektroUgMontazh" company. The following equipments have been used during measurement:

- an arbitrary waveform generator Г3-112/1. This equipment is a source of sinusoidal (basic mode) and rectangular (optional mode) signals intended for research, configure, and test systems and devices used in electronics, communications, automation, computing and measurement techniques. It produces 20 Vp-p sinusoid with frequency range of 0-80 MHz;
- analog oscilloscope C1-99. Oscilloscope designed for observation and measurement of electrical signals in the frequency band from 0 to 50 MHz, is applied in the laboratory, plant and field conditions;
- LCR bridge and multimeter The effective inductance and ground capacitance were measured by an LCR bridge at 1 kHz, while the dc resistance was measured by a multimeter.

2.3.1 Measurement method

Algorithm of performing measurement:

Step 1. Construct scheme according to the Figure 2.2;
Step 2. Turn on generator to 50 Hz, configure the oscilloscope;
Step 3. Measure input voltage and output voltage, compare the obtained result with the expected as in (2.2):

$$k = \frac{V_{in}}{I_{out}}, \tag{2.2}$$

where k – transformation coefficient;
V_{in} – input voltage;
I_{out}- output current.

Step 4. Switch generator to 10 kHz;
Step 5. Measure V_{in} and I_{out};
Step 6. Enter oscilloscope indications to the measurement table;
Step 7. Increase the frequency by 10 kHz;
Step 8. Repeat step 5-7;
Step 9. Complete measurement when frequency riches 1 MHz;
Step 10. Repeat step 1-10 for other phases of transformer winding;
Step 11. Construct resultant frequency characteristics.

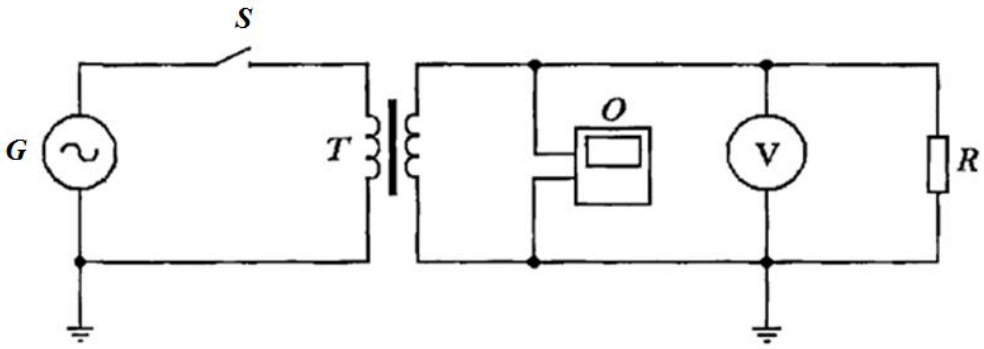

G – generator Г3-112/1, S – switch, T – transformer, V – control voltmeter, R– load resistance

Figure 2.2 – scheme of measurement performance (single phase)

2.3.2 Analysis of obtained frequency characteristics of transformer winding

FRA was performed on the 11-kV winding of a two-winding transformer (315 kVA, 11/6.9 kV) with its neutral grounded, while the other winding was short-circuited and grounded. The measured values of DC resistance and efficient inductance are 2.2 Ω and 22.4 mH, respectively. Measurement method described above was conducted on this transformer and obtained FRA plots are shown in Figure 2.3.

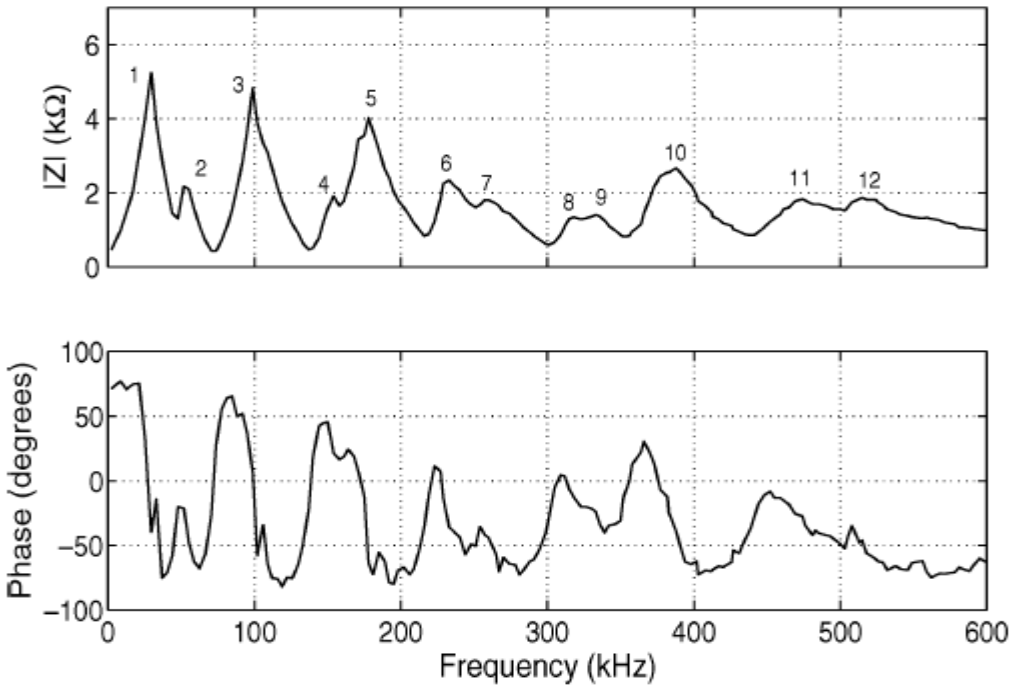

Figure 2.3 – Measured FRA on a 315 kVA, 11/6.9kV transformer

3 Modeling a transformer winding

In this chapter, the modeling of a transformer winding is demonstrated. FRA technique is used as a methodology to solve problems in winding deformation detection. Applicability of ladder network representation of model winding is discussed.

Investigation was conducted on model winding consisted of a single-layer wound on an insulated air-core former of diameter 200 mm. The winding had 200 turns and taps were provided after every 20 turns. Continuous disk winding is presented using these taps and by connecting series and shunt capacitances.

For this research, frequency range of interest from 10 kHz to 2 MHz is chosen. From the operational requirement, the type and location of faults are imperative.

In the FRA technique, a low amplifier swept frequency signal is applied at the end of one of the transformer windings and the response is measured at the other end of the winding with one phase at a time. Method consists of measuring the impedance of transformer winding over a wide range of frequencies and comparing the results of these measurements with a reference set taken during installation. Difference in the signature of the frequency response indicates damage to the transformer, which is examined internally by investigating resultant bode plots.

3.1 Equivalent Circuit of model winding

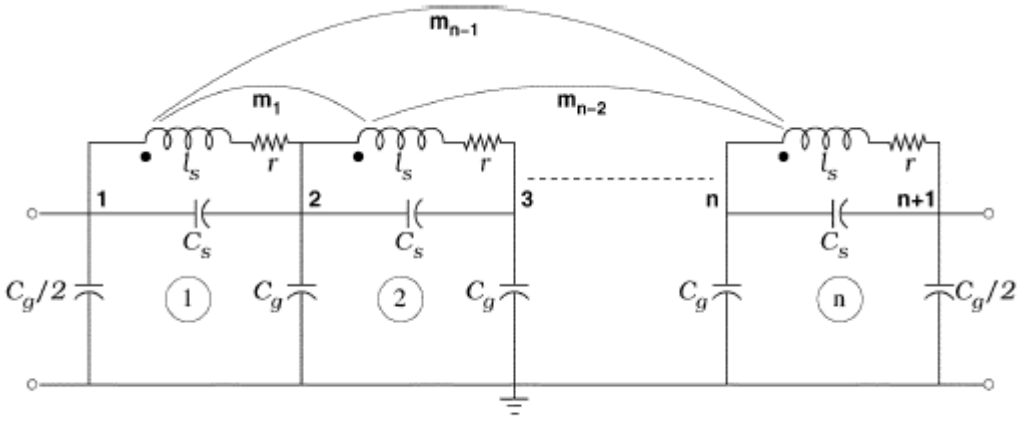

Figure 3.1 – Equivalent circuit of a transformer winding

Representation of model winding as an electrical circuit helps to inherently capture the physical length of the winding (Figure 3.1). Or, in other words, the physically continuous winding can be visualized as being mapped onto a series of discrete nodes, starting from line to neutral end.

The synthesized circuit should exhibit the same terminal characteristics as that of the model winding (i.e., difference between all their corresponding short

circuit natural frequencies (scnf) and open-circuit natural frequencies (ocnf) should be within a specified tolerance).

3.1.1 Synthesize Reference Circuit

The first step in the proposed method involves representing the model winding by means of an equivalent circuit, called the reference circuit. To achieve this, the following quantities of the model winding are required:

- dc resistance R_{DC};
- equivalent air-core inductance L_{eq};
- effective shunt capacitance to ground $C_{g,eff}$;
- initial voltage distribution constant α .

Among these, the quantities R_{DC}, L_{eq} and $C_{g,eff}$ are measurable at the input terminals of the model and the initial voltage distribution constant (α) can be got from design details. The steps involved in synthesizing a circuit to represent the model winding are as follows:

a) determine natural frequencies (ocnfs and scnfs) of the model winding by swept frequency measurements;

b) Determine the number of sections of the equivalent circuit to be synthesized;

c) Estimate individual values of the elements of the equivalent circuit.

Each of these steps is discussed below:

a) Determine Natural Frequencies. The driving-point impedance function of an n-section equivalent circuit (as in Fig. 1) with its neutral grounded can be expressed as [24]

$$Z(s) = \frac{\beta_1 (s-\tau) \prod_{i=1}^{n-1} (s-z_i)(s-\acute{z_i})}{\prod_{i=1}^{n} (s-p_i)(s-\acute{p_i})}, \qquad (3.1)$$

where β_1- scaling factor;

τ - real zero;

$z_i, \acute{z_i}$ - complex conjugate zero pair;

$p_i, \acute{p_i}$ - complex conjugate pole pair.

Poles and zeros of the driving-point impedance function lie in the left half of the complex frequency plane. For driving-point functions, in the complex poles $(\delta_p + jw_p)$ and complex zeros $(\delta_z + jw_z)$, the real parts are due to the losses (represented as resistances) and the imaginary parts signify the angular frequencies at which the peaks and troughs occur in the magnitude plot of the driving-point function;

b) Natural Frequencies Pertaining to Second-Order Poles and Zeros. To determine the natural frequencies of the model winding, swept frequency measurements are performed on it. This essentially involves varying the excitation frequency over a wide range and at every frequency, the magnitude and phase of the input voltage and current are measured, using which the driving-point impedance is determined.

The measured magnitude and phase plots of the driving-point impedance corresponding to a continuous-disc model winding are presented in Figure 3.2 [25]. From this figure, the following points emerge:

- at certain frequencies, the magnitude of the driving-point impedance becomes maximum and simultaneously its phase becomes zero (while changing from positive to negative). These frequencies are referred as open-circuit natural frequencies (ocnf f_p's);

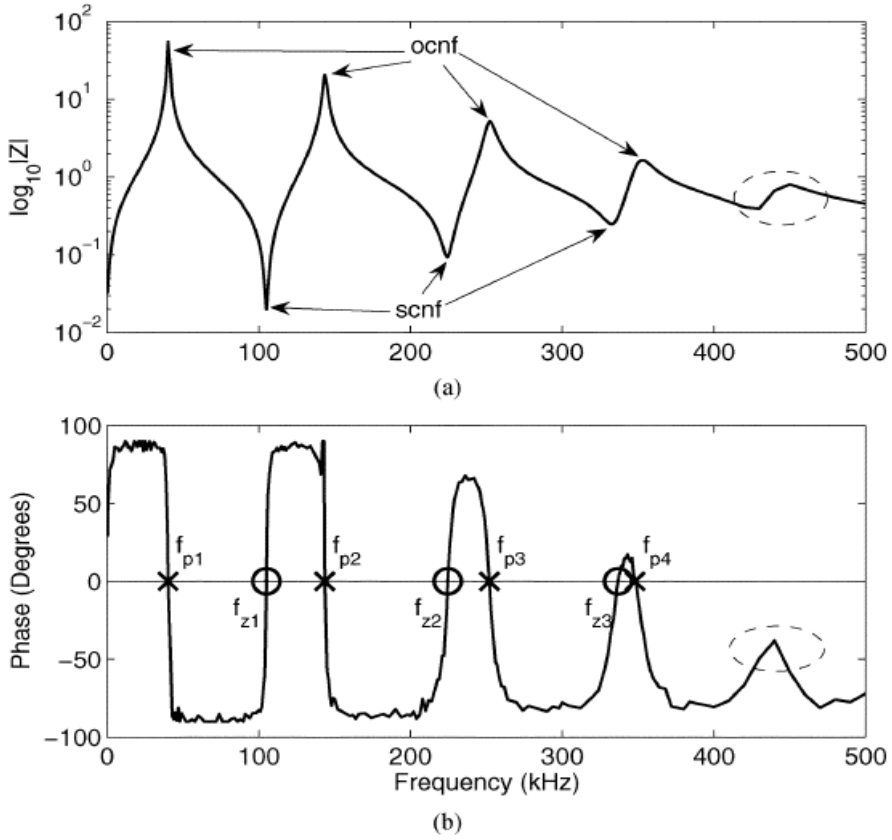

Figure 3.2 – Measured driving-point impedance of the model (a) magnitude and (b) phase

- at some frequencies, the magnitude of the driving-point impedance becomes minimum and its phase simultaneously becomes zero (while changing from negative to positive), and these frequencies are referred as short-circuit natural frequencies (scnf f_z's).

Thus, ocnfs and scnfs pertaining to the second-order poles and zeros of driving-point impedance function can be determined by inspection of the magnitude and phase plots;

c) Natural Frequency (scnf) Pertaining to First-Order Zero. The driving-point impedance function (3.1) contains a real zero τ (where, $\tau = -2\pi f_1$). As the loss is generally very low, the scnf 'f_1' would lie in the low-frequency region (of the order of a few hundreds of hertz) and it can be determined as follows.

The impedance $Z(s)$ at low frequencies is

$$\lim_{s\to 0} Z(s) = R_{DC} + sL_{eq}\ , \tag{3.2}$$

where R_{DC} – DC resistance;
L_{eq} – equivalent inductance;
s – Laplace variable;
Z(s) – impedance.

From the above, the real zero ($s = \tau$) is found to be

$$\tau = -\frac{R_{DC}}{L_{eq}}, \tag{3.3}$$

where R_{DC} – DC resistance;
L_{eq} – equivalent inductance;
τ – real zero.

d) Determine the Number of Sections *N*. While synthesizing the circuit, determination of the number of sections *N*, is very crucial. For estimating it, the rule-of thumb mentioned in [26] can be used (i.e., "the number of sections to be used in the equivalent circuit can be chosen somewhat larger than the required number of natural frequencies"). From this, at first glance it appears as though the determination of *N* from the magnitude plot is straightforward. However, this is true, if and only if all the natural frequencies are observable. But in practice, not all of them are observable, because of the following reasons:

- at higher frequencies, due to skin-effect, damping is high. Hence, the high frequency scnfs and ocnfs are not well-pronounced in the frequency response plots (Figure 3.2). Thus, the true value of (minimum number of sections the equivalent circuit should have to reproduce the same terminal characteristics as that of the winding) cannot be ascertained based on a mere count of the number of peaks and troughs;

- corresponding to ocnf (or peaks in the magnitude plot), the current drawn from the source would approach zero. This makes it difficult to differentiate between signal and noise, in spite of adopting signal averaging techniques afforded by digital oscilloscopes. Further, it also becomes increasingly difficult to precisely identify a zero crossing of the phase angle;

- in an interleaved winding, since most of the high-frequency zeros and poles lie very close to each other, only a few natural frequencies are observable in the

frequency response plots [27]. In such cases, determining the true value of *N* based only on an inspection of the frequency-response plots is not possible;

- further, in actual measurements, the frequency response plots exhibit a few tiny peak-like kinks. These artifacts are due to noise, limited sensitivity of the measuring instruments, etc. Hence, estimation of *N* is fraught with difficulties;

- sometimes, a well-defined trough/peak may occur in the magnitude plot, but the corresponding phase may not attain zero. Such frequencies will not be considered as scnf/ ocnf. One example is seen in Figure 3.2, wherein the encircled trough/peak has not been considered as scnf/ocnf.

Due to the above reasons, the number of clearly identifiable peaks is always less than *N* (i.e., *q* peaks and (*q*-1) troughs). Utilizing this limited information, how the value of can actually be arrived at is discussed next.

At high frequencies, the impedance offered by the circuit is found from (3.1) as

$$\lim_{s\to\infty} Z(s) = \frac{\beta_1}{s}, \tag{3.4}$$

where s – Laplace variable;
Z(s) – impedance;
β_1 – scaling factor.

Since, the circuit behaves entirely as a capacitive network at higher frequencies, the scaling factor β_1 can be related to the equivalent capacitance C_{eq} as

$$\beta_1 = \frac{1}{C_{eq}} \tag{3.5}$$

where β_1 – scaling factor;
C_{eq} – equivalent capacitance.

The above relation is a crucial link which can be made use for determining *N*.

At $s = 0$, the input impedance becomes resistive (i.e., R_{DC}). Using this and substituting (3.3) in (3.1), the scaling factor β_1 can be expressed as

$$\beta_1 = L_{eq} \times \frac{\prod_{i=1}^{n}(-p_i)(-\acute{p_i})}{\prod_{i=1}^{n-1}(-z_i)(-\acute{z_i})}, \tag{3.6}$$

where β_1 – scaling factor;
L_{eq} – equivalent inductance;
$z_i, \acute{z_i}$ - complex conjugate zero pair;
$p_i, \acute{p_i}$ - complex conjugate pole pair.

Since only *q* ocnfs and (*q-1*) scnfs are observable, *n* and (*n-1*) in the above equation can be replaced by *q* and (*q-1*) , respectively.

Also, as the absolute value of the imaginary parts of complex frequencies is significantly higher than their real parts (losses in the winding are low), p_i's and z_i's in (3.6) can be replaced by the angular frequencies w_p's and w_z's, respectively. Since imaginary parts of poles and zeros are $w_p = 2\pi f_p$ and $w_z = 2\pi f_z$, respectively, (3.6) can be rewritten as

$$\beta_1 \approx L_{eq} \times \frac{4\pi^2 \prod_{i=1}^{q} f_{pi}^2}{\prod_{i=1}^{q-1} f_{zi}^2}, \tag{3.7}$$

where β_1 – scaling factor;
L_{eq} – equivalent inductance, in mH;
$z_i, \acute{z}_i$ - complex conjugate zero pair, in MHz;
$p_i, \acute{p}_i$ - complex conjugate pole pair, in MHz.

One of the unique properties of driving-point impedance function [22] is that its poles and zeros alternate with each other. That is, every trough (complex conjugate zero pair) alternates with a peak (complex conjugate pole pair). Further, the number of peaks is more than the troughs by unity. (Note: This feature is not exhibited by the transfer function and hence instead of it the driving-point impedance function was chosen in this study.)

From Figure 3.2(b), by inspection, it can be inferred that the ratio of the square of any ocnf to that of the preceding scnf is always greater than unity. Hence, if a ocnf-scnf pair (or peak-trough pair) is not accounted for (due to the reasons mentioned before), then the value of β_1 estimated with reduced number of ocnfs and scnfs will always be less than its actual value and, hence, (3.5) would become modified as

$$\left(\frac{1}{C_{eq}} - \beta_1\right) > 0, \tag{3.8}$$

where β_1 – scaling factor;
C_{eq} – equivalent capacitance.

The above inequality forms the basis for finding and the steps involved for its estimation are given in Algorithm 1.

Algorithm 1. Determining Number of Sections

Step 1. Measure oscnf $\{f_{pi}, \quad \forall i = 1, \ldots, q\}$ and scnfs $\{f_{zi}, \quad \forall i = 1, \ldots, q-1\}$ of the model winding;
Step 2. Determine β_1 using equation (3.7);
Step 3. $N \leftarrow q$;
Step 4.

$$C_g = \frac{C_{g,eff}}{N}\ ; \qquad C_s = \frac{C_{g,eff} \times N}{\alpha^2}. \tag{3.9}$$

Step 5. Estimate C_{eq} of ladder network with *N* sections as

$$C_{eq} = \frac{C_g}{2} + \frac{1}{\frac{1}{C_s} + \frac{1}{C_g + \frac{1}{\frac{1}{C_s}+\cdots}}}\ . \tag{3.10}$$

Step 6. **if** $\left(\left(\frac{1}{C_{eq}} - \beta_1\right) < 0\right)$, **then**

Step 7. $N \leftarrow N + 1$.

GOTO step 4

Step 8. **end if**

e) Determine Elements of Reference Circuit:

- Capacitances and Resistances. From the values of C_g and C_s (capacitances per section) determined in (3.9), the nodal capacitance matrix $[K_{ref}]$ can be constructed. Further, the sectional value of the resistance can be determined as

$$r = \frac{R_{DC}}{N}, \tag{3.11}$$

where $R_{DC} -$ DC resistance;

N – number of section;

r – resistance value per section.

Let $[R_{ref}]$ be the diagonal matrix with its elements equal to *r;*

- Inductances. Let be the self-inductance of the first section and $m_1, m_2, \ldots, m_{N-1}$ be the mutual inductances between the first and the other sections in the circuit, respectively. The magnetic coupling between individual sections decreases when their separation distance increases. So it is logical to consider that the self and mutual inductances satisfy the following constraints:

$$\begin{aligned} 0.4\, l_s < m_1 < 0.8\, l_s \\ 0.4\, m_{i-1} < m_i < 0.8\, m_{i-1}\,, \quad \forall i = 2, \ldots, N-1 \end{aligned} \tag{3.12}$$

The limits, namely 0.4 and 0.8, were found to be suitable in this work and can be changed, if needed. Assuming symmetry, the remaining self and mutual inductances can be taken to be the same. The inductance matrix [L] is constructed such that its diagonal elements are equal to the values of the self inductances, and the nondiagonal elements are the mutual inductances. The estimation of mutual inductances can be accomplished by imposing (3.12) and following an iterative procedure as explained in Algorithm 2. (Note: In case, if the symmetry does not exist, then a similar constraint as in (3.12) can be chosen for the other sections also).

Algorithm 2. Determining inductances of the reference circuit

Step 1. $\{l_s,\ m_1, m_2, \ldots, m_{N-1}\} \leftarrow$ minimum values as per equation (3.12);
Step 2. Increase the value of one inductance by 1% of l_s (either self or mutual) and estimate the equivalent inductance as

$$L_{eq}(estimated) = Nl_s + 2\sum_{i=1}^{N-1}(N-i)m_i \qquad (3.13)$$

Step 3. **if** $(L_{eq}(estimated) \approx L_{eq},\ within\ 1\%\ tolerance)$ **then**
Step 4. Construct inductance matrix [L];
Step 5. Estimate ocnfs $\{f_{pi}, \forall i = 1, \ldots, N\}$ and scnfs $\{f_{zi}, \forall i = 1, \ldots, N-1\}$ using $[K_{ref}]$, $[R_{ref}]$, [L];
Step 6. **if** $\left(estimated\left\{f_p, f_z\right\} \approx measured\left\{f_p, f_z\right\}, within\ 1\%\ tolerance\right)$ **then**
Step 7. $[L_{ref}] = [\mathrm{L}]$;
Step 8. **else**
Step 9. GOTO step 2;
Step 10. **end if**
Step 11. **else**
Step 12. GOTO step 2
Step 13. **end if**

Thus, $[K_{ref}]$, $[R_{ref}]$ and $[L_{ref}]$ correspond to the reference circuit. These will be subsequently used as initial guess to synthesize further circuits, when changes are introduced in the model winding. Refer to Appendix A to see calculated values of $[K_{ref}]$, $[R_{ref}]$ and $[L_{ref}]$.

3.2 Mathematical model of transformer winding

Construction of mathematical model of winding contains following steps:

a) Definition. The state of a system may be considered as the least amount of information that must be known about the given system at a given time to determine its subsequent dynamics completely. A suitable selection of the independent variables result in a set of first order differential equations that are linearly independent [9]. These variables and equations are known as state variables and state equations respectively.

The most general form of the state equations of a linear, time invariant network is as follows:

State equation: $\dot{\boldsymbol{x}}$= [A] **x** + [B]**u** (3.14)
Output equation: **y** = [C] **x** + [D]**u** (3.15)

where **x** - column vector of the state variables;

$\dot{\boldsymbol{x}}$- time derivatives of the state variables;

u- excitation or input vector;

y - response or output vector;

{[A]; [B]; [C]; [D]} - matrices of constant coefficients.

b) Choice of State Variables. For a system to be analyzed, though the selection of state variables is not unique, they are to be chosen so as to enable formulation of state equations with least effort. A random selection of state variables may increase the complexity of the solution methodology and may also result in redundant equations. To avoid such situations, there exist some guidelines for selecting the state variables.

In physical terms, the state variables specify the energy stored in a set of independent energy storage elements. It is thus natural that, the number of state variables should be equal to the number of energy storing elements of the network, provided there are no tie sets of capacitors and cut sets of inductors. As the circuit model (Figure 3.1) has tie sets of capacitors within the winding and between the windings, the count of state variables is less than the number of energy storing elements by the number of capacitance tie sets [20].

Based on this rationale, the currents through inductances and voltages across shunt capacitances (excluding the capacitance across the line terminal and datum of the primary winding) are chosen as the desired set of state variables. Since voltage across any series or interwinding capacitance can be expressed in terms of the nodal voltages, voltages across these capacitances are excluded from the list of state variables.

For the circuit model shown in Figure 3.1, the state variables are assigned as below:

a) inductor currents of the primary winding: $i_1,\ i_2, ..., i_n$;

b) nodal voltages of the primary winding (excluding the line end which is energised by the source): $e_2, e_3, ..., e_n$.

Since, voltage across an inductor or current through a capacitor is governed by a first order differential equation, the formulation of the state equations becomes straightforward with the choice of these state variables;

c) State Model Formulation. State equations are to be formulated for the primary winding of a two winding transformer (Figure 3.1) whose secondary is short circuited. The objective here is to express the derivatives of the state variables in terms of the state variables and the excitation.

- Time Derivatives of the Inductor Currents. Let $v_1, v_2, v_3, \ldots v_n$ denote the voltages across the inductances of the primary circuit.

Let $[L]$ represent the self and mutual inductance matrix of the circuit. Since, time derivatives of the inductance currents are related to the voltages across the inductances as,

$$\begin{bmatrix} di_1/dt \\ di_2/dt \\ \vdots \\ di_n/dt \end{bmatrix} = [L]^{-1} \begin{bmatrix} v_1 \\ v_2 \\ \vdots \\ v_n \end{bmatrix} \tag{3.16}$$

where, $[L]^{-1}$ inverse matrix of $[L]$. Since, the voltage across the inductances can be expressed in terms of the nodal voltages, the above gets modified to,

$$\begin{bmatrix} di_1/dt \\ di_2/dt \\ di_n/dt \end{bmatrix} = [L]^{-1} \begin{bmatrix} e_1 - e_2 - i_1 r \\ e_2 - e_3 - i_2 r \\ e_n - i_n r \end{bmatrix} \tag{3.17}$$

Let $[R]$be a diagonal matrix with its element equal to the sectional value of the resistance `r'.

$$R(i,i) = r, \qquad 1 \le i \le n \tag{3.18}$$

Expressing the inductor voltages in terms of node voltages and the resistive voltage drops, the above equation gets modified to the following form,

$$\begin{bmatrix} di_1/dt \\ di_2/dt \\ \vdots \\ di_n/dt \end{bmatrix} = [L]^{-1} \begin{bmatrix} e_1 - e_2 \\ e_2 - e_3 \\ \vdots \\ e_n \end{bmatrix} + [L]^{-1} \begin{bmatrix} -i_1 r \\ -i_2 r \\ \vdots \\ -i_n r \end{bmatrix} = [L]^{-1}[T]^t \begin{bmatrix} e_1 \\ e_2 \\ \vdots \\ e_n \end{bmatrix} - [L]^{-1}[R] \begin{bmatrix} i_1 \\ i_2 \\ \vdots \\ i_n \end{bmatrix} \tag{3.19}$$

[T] matrix has the following form:

$$[T] = \begin{bmatrix} 1 & 0 & \cdots & 0 & 0 \\ -1 & 1 & \cdots & 0 & 0 \\ \vdots & \vdots & & \vdots & \vdots \\ 0 & 0 & \cdots & -1 & 1 \end{bmatrix} \tag{3.20}$$

Assigning $[I_e]$ = - $[L]^{-1}$ $[T]^t$ and $[I_i]$ = - $[L]^{-1}$[R], equation becomes,

$$\begin{bmatrix} di_1/dt \\ di_2/dt \\ \vdots \\ di_n/dt \end{bmatrix} = [I_e] \begin{bmatrix} e_1 \\ e_2 \\ \vdots \\ e_n \end{bmatrix} + [I_i] \begin{bmatrix} i_1 \\ i_2 \\ \vdots \\ i_n \end{bmatrix} \tag{3.21}$$

- Time Derivatives of the Nodal Voltages. Applying KCL (Kirchhoff's current law) to the circuit of Figure 3.1, that is, the sum of the currents diverging from the nodes through the inductances and the capacitancesequals the currents fed to the nodes, results in,

$$\begin{bmatrix} i_1 \\ i_2 - i_1 \\ \vdots \\ i_n - i_{n-1} \end{bmatrix} + [K] \begin{bmatrix} de_1/dt \\ de_2/dt \\ \vdots \\ de_n/dt \end{bmatrix} = 0 \tag{3.22}$$

Where, [K] represents the node capacitance matrix of the circuit. The above equation can be written as,

$$[K] = \begin{bmatrix} C_s + C_{g1}/2 & -C_s & \cdots & 0 \\ -C_s & 2C_s + C_{g2} & \cdots & 0 \\ & \vdots & & \vdots \\ 0 & 0 & \cdots & 2C_s + C_{gN} \end{bmatrix} \tag{3.23}$$

$$[T] \begin{bmatrix} i_1 \\ i_2 \\ \vdots \\ i_n \end{bmatrix} + [K] \begin{bmatrix} de_1/dt \\ de_2/dt \\ \vdots \\ de_n/dt \end{bmatrix} = 0 \tag{3.24}$$

Assigning [Ei] = - $[K]^{-1}$ [T], time-derivatives of node voltages can be expressed as,

$$\begin{bmatrix} de_1/dt \\ de_2/dt \\ \vdots \\ de_n/dt \end{bmatrix} = [E_i] \begin{bmatrix} i_1 \\ i_2 \\ \vdots \\ i_n \end{bmatrix} \tag{3.25}$$

d) State equation. By merging equations (3.21) and (3.25), state equation corresponding to the circuit in Figure 3.1, is obtained as,

$$\begin{bmatrix} de_1/dt \\ \vdots \\ de_n/dt \\ di_1/dt \\ \vdots \\ di_n/dt \end{bmatrix} = \left[\begin{array}{c|c} 0 & E_i \\ \hline I_e & I_i \end{array}\right] \begin{bmatrix} e_1 \\ \vdots \\ e_n \\ i_1 \\ \vdots \\ i_n \end{bmatrix} \tag{3.26}$$

The above equation can also be expressed as,

$$\dot{\mathbf{x}} = [A]\,\mathbf{x} \tag{3.27}$$

e) Output Equation. Neutral current of the primary winding is chosen as the output variable "y" of the state model, so it is to be expressed in terms of the state variables (x) and the input (u).

From Figure 3.1, it is obvious that, neutral current is the sum of the currents through the inductance and the series capacitance of *n*th section of the primary winding, that is,

$$i = i_n + C_s \frac{de_n}{dt} \tag{3.28}$$

Using the definition of state variables and making use of (3.27), the above equation can be rewritten as,

$$y = x_n + C_s([A_y]x + [B_y]u) \tag{3.29}$$

where, $[A_y]$ and $[B_y]$ represent *n*th row of [A] and [B] respectively. The first two terms of the above equation can be merged together by assigning $[C]x = x_n + C_{s[A_y]}\,x$ and let $D = C_s[B_y]$. Now, (3.2.16) modifies to,

$$y = [C]x + [D]u \tag{3.30}$$

Thus, the output variable of the state model is expressed in terms of the state variables and the input vector. Equations (3.27) and (3.30) together constitute the state model of the network.

3.2.1 Determination of TF poles and zeros

To find an analytical expression for transfer function, the time domain state equations are to be transformed to s-domain.

Applying Láplace transform to (3.27) and (3.30), and simplifying them, leads to,

$$Y(s) = ([C][sI - A]^{-1}[B] + [D])U(s) \tag{3.31}$$

where, is an identity matrix of dimension same as that of [A] .

Since,

$$L(u) = U(s) = \begin{bmatrix} 1 \\ s \end{bmatrix} E_1(s) \tag{3.32}$$

Transfer function, which is defined as a ratio of the output $Y(s)$ to the input voltage , is obtained as,

$$TF = \frac{Y(s)}{E_1(s)} = ([C][sI - A]^{-1}[B] + [D]) \begin{bmatrix} 1 \\ s \end{bmatrix} \tag{3.33}$$

Using the above equation, it is possible to obtain a plot of TF by assigning numerical values to *s* (*s* = *jw*, complex frequency) over a wide range of frequencies. As already mentioned, such a plot will not directly yield the complete information of all the poles and zeros of TF.

Conversion of state space model to transfer function form. Process includes following steps:

a) Mathematical Intricacies in Computing TF. The evaluation of TF as per (3.33) requires the computation of the inverse of a symbolic matrix $[sI - A]$ which has symbolic variable s. Finding $[sI - A]^{-1}$ needs large time, even when [*A*] is small. Hence, a method is explored for circumventing this bottleneck.

Finding the inverse of a matrix becomes a much simpler operation, if and only if, the matrix is diagonal. It is because the inverse of such matrix is a diagonal matrix, whose diagonal elements are just the reciprocal of the diagonal elements of the matrix. With this in mind, the existing state model needs to be transformed into another state model, where the system matrix will be diagonal in nature;

b) Diagonalization of System Matrix. Diagonalising the system matrix can be achieved through linear transformation, a well known technique [23]. It is to be mentioned that, the transfer function is invariant through linear transformation. If the basis of the vector space is changed through a transformation matrix constructed from the eigenvectors of the system matrix [*A*], then it will result in a state model, whose system matrix will be diagonal.

Eigenvalues $\lambda_1, \lambda_2, \ldots \lambda_v$ of the system matrix are determined, from which the transformation matrix ([M], called modal matrix) is constructed such that, its columns are the eigenvectors of [*A*]. By performing linear transformation, $= [M]z$, (3.27) and (3.30) get transformed to,

$$\dot{z} = [\Lambda]z + [\tilde{B}]u \quad (3.34)$$
$$y = [\tilde{C}]z + [\mathrm{D}]u \quad (3.35)$$

where $[\Lambda] = [M]^{-1}[A][M]$;
$[\tilde{B}] = [M]^{-1}[B]$ *and* $[\tilde{C}] = [C][M]$.

It is to be mentioned here that, $[\Lambda]$ is a diagonal matrix whose elements are same as the eigenvalues $\lambda_1, \lambda_2, \ldots \lambda_v$ of $[A]$. Equations (3.34) and (3.35) are now referred as the transformed state model of the network considered. TF of the system is obtained by using (3.33) with matrices replaced $([A], [B], [C], [D])$ replaced by $([\Lambda], [\tilde{B}], [\tilde{C}], [D])$ as below,

$$TF = ([\tilde{C}][sI - \Lambda]^{-1}[\tilde{B}] + [D])\begin{bmatrix}1\\ s\end{bmatrix} \quad (3.36)$$

$[sI - \Lambda]$ is a diagonal matrix. Although $[sI - \Lambda]^{-1}$ is computed efficiently, the symbolic variable still continues to remain in the TF expression and poses problems, especially when larger networks are considered. A means of elimination of from the actual computation process will be examined next;

c) Algebraic Method of Constructing TF. The procedure of constructing TF by means of extracting the coefficients of the numerator and denominator polynomials is explained here. Of the matrices involved in the TF expression, the only symbolic matrix is $[sI - \Lambda]^{-1}$, which is diagonal and the rest of them are numeric in nature. This diagonal form easily lends itself to algebraic manipulation, yielding the coefficients of numerator and denominator polynomials of TF. Once the coefficients of these polynomials are obtained, then it becomes straightforward to find their roots (poles and zeros). This manipulation is a crucial step and is explained below.

The transformed state model is characterized by the matrices $([\Lambda], [\tilde{B}], [\tilde{C}], [D])$ and they are of the form,

$$[\Lambda] = \begin{bmatrix}\lambda_1 & 0 & \cdots & 0\\ 0 & \lambda_2 & & 0\\ \vdots & & \ddots & \vdots\\ 0 & 0 & \cdots & \lambda_v\end{bmatrix}, \qquad [\tilde{B}] = \begin{bmatrix}b_{11}\\ b_{21}\\ \vdots\\ b_{v1}\end{bmatrix},$$

$$[\tilde{C}] = [c_1 \quad c_2 \quad \cdots \quad c_v], \qquad [D] = [d_1]. \quad (3.37)$$

The inverse of the characteristics matrix becomes,

$$[sI-\Lambda]^{-1}=\begin{bmatrix}\frac{1}{s-\lambda_1} & 0 & \cdots & 0\\ 0 & \frac{1}{s-\lambda_2} & \cdots & 0\\ \vdots & \vdots & \ddots & 0\\ 0 & 0 & \cdots & \frac{1}{s-\lambda_v}\end{bmatrix}, \tag{3.38}$$

Let $[\Delta(s)]=\left[\tilde{C}\right][sI-\Lambda]^{-1}[\tilde{B}]$ and is evaluated as,

$$[\Delta(s)]=\begin{bmatrix}\frac{c_1}{s-\lambda_1} & \frac{c_2}{s-\lambda_2} & \cdots & \frac{c_v}{s-\lambda_v}\end{bmatrix}\begin{bmatrix}b_{11}\\ b_{21}\\ \vdots\\ b_{v1}\end{bmatrix}, \tag{3.39}$$

The above can be simplified to,

$$[\Delta(s)]=[\delta(s)], \tag{3.40}$$

where,

$$[\delta(s)]=\frac{b_{11}c_1}{s-\lambda_1}+\frac{b_{21}c_2}{s-\lambda_2}+\cdots+\frac{b_{v1}c_v}{s-\lambda_v}=\frac{\alpha_1(s)}{\beta(s)} \tag{3.41}$$

with, $\alpha_1(s)\ and\ \beta(s)\ expressed\ as,$

$$\alpha_1(s)=\sum_{i=1}^{v} b_{i1}c_i\prod_{j=1,j\neq i}^{v}(s-\lambda_j) \tag{3.42}$$

$$\beta(s)=\prod_{i=1,}^{v}(s-\lambda_i), \tag{3.43}$$

Equation (3.36) can be written as,

$$TF=([\Delta(s)]+[D])\begin{bmatrix}1\\ s\end{bmatrix}, \tag{3.44}$$

Substituting for $[\Delta(s)]$ and $[D]$ and simplifying the above equation results in,

$$TF=\frac{\alpha_1(s)+d_1\beta(s)}{\beta(s)}=\frac{P(s)}{Q(s)}, \tag{3.45}$$

where $P(s)$ and Q(s) represent the numerator and denominator polynomials of TF respectively;

d) Determination of Poles. Poles of TF are the roots of the polynomials Q(s). Referring to (3.43) and (3.45) yields,

$$Q(s) = \prod_{i=1,}^{v}(s - \lambda_i), \tag{3.46}$$

Therefore, poles of TF are $\lambda_1, \lambda_2, \ldots \lambda_v$ which are same as eigenvalues of the system matrix $[A]$ and have already been determined;

e) Determination of Zeros. Zeros of TF are the roots of the polynomial P(s). From (3.45),

$$P(s) = \alpha_1(s) + d_1\beta(s), \tag{3.47}$$

Coefficients of the polynomial $P(s)$ can be obtained through the algebraic manipulation of the coefficients of polynomials $\alpha_1(s)\ and\ \beta(s)$ which can be extracted, as illustrated below.

Referring to (3.43), since $\beta(s)$ is expressed as the product of *v* factors (each of the form $(s - \lambda_i)$), the extraction of coefficients from the polynomial $\beta(s)$ having $\lambda_1, \lambda_2, \ldots \lambda_v$ as its roots becomes a simple task (a built-in function for extracting coefficients of a polynomial with known roots, 'poly' exists in Matlab). The order of *s* in the polynomial $\beta(s)$ is *v* and hence the extracted values will correspond to the coefficients of $s^v, s^{v-1}, \ldots, s^1, s^0$ in the polynomial $\beta(s)$.

Similarly, coefficients of the polynomial $\alpha_1(s)$ can also be extracted from (3.42). The order of *s* in these polynomials is *v-1* and hence the extracted values will correspond to the coefficients of $s^{v-1}, s^{v-2}, \ldots, s^1, s^0$ the polynomial. Therefore, the extracted coefficients of the polynomials can be expressed in a form shown below,

$$\begin{matrix} \textit{Polynomial} \\ \begin{bmatrix} \beta(s) \\ \alpha_1(s) \end{bmatrix} \end{matrix} \rightarrow \begin{matrix} \textit{coefficients} \\ \begin{bmatrix} \beta^v & \beta^{v-1} & \cdots & \beta^1 & \beta^0 \\ & \alpha_1^{v-1} & \cdots & \alpha_1^1 & \alpha_1^0 \end{bmatrix} \end{matrix} \tag{3.48}$$

Coefficients of $P(s)$ can be constructed easily from (3.48). Summation of the coefficients of like powers of s of the polynomials involved in $P(s)$ yields the coefficients of $P(s)$.

Since zeros and poles of TF are computed through manipulation of the matrices which are numeric in nature, without involving any symbol, the process will require lesser computing time and memory. Thus, an entirely symbol-free computation of poles and zeros of TF has been achieved.

3.3 Simulation of model winding

Capacitive changes were made in the transformer winding, and reflection of that changes were examined on a model winding constructed using Simulink. The ability of the proposed method to correctly locate the position and extent of the change introduced as in Table 3.1.

Table 3.1 – Measured and Estimated Frequencies after changes

Case	Measured with transformer winding		Estimated using simulation model	
	scnf (kHz)	ocnf (kHz)	scnf (kHz)	ocnf (kHz)
A1	104.97 224.80 336.15	38.80 138.90 247.00 343.54	105.19 224.81 334.47 410.02 472.45	39.00 138.33 245.20 344.02 413.35 473.49
	$C_g'(1,0): 0.28 \rightarrow 0.5$		$C_g(1,0): 0.467 \rightarrow 0.65$	
A2	97.95 224.68 327.1	39 138.2 250.6 340.2	98.76 224.81 325.45 410.02 465.18	39.28 137.83 248.76 337.96 414.15 466.95
	$C_g'(6,0): 0.56 \rightarrow 1.06$		$C_g(4,0): 0.933 \rightarrow 1.35$	
A3	105.5 227.9 343.7	40.30 144.30 254.80 354.89	106.10 229.40 341.83 416.58 475.35	40.55 144.17 254.39 353.36 420.30 476.50
	$C_g'(10,0): 0.56 \rightarrow 1$		$C_g(6,0): 0.933 \rightarrow 0.67$	
A4	104.33 221.26 327.4	37.20 138.30 249.43 346.20	103.79 217.93 324.98 403.81 470.14	37.49 139.35 247.19 340.25 408.29 471.44
	$C_g'(2,0): 0.56 \rightarrow 1.06$		$C_g(1,0): 0.467 \rightarrow 0.667$ $C_g(2,0): 0.933 \rightarrow 1.333$	
B1	101.3 216.7 331	38.4 144.6 246.8 341	101.52 219.54 337.52 414.08 472.73	39.15 143.68 244.74 346.82 417.71 473.75
	$C_s'(3,4): 1 \rightarrow 0.56$ $C_g'(4,0): 0.56 \rightarrow 1$		$C_s(2,3): 0.6 \rightarrow 0.5$ $C_g(3,0): 0.933 \rightarrow 1.283$ $C_g(2,0): 0.933 \rightarrow 0.883$	
B2	105.06 218.98 334.4	40.1 144.1 242.1 353	105.60 220.23 335.07 405.87 473.61	40.22 144.88 241.31 350.90 407.70 475.65
	$C_s'(5,6): 1 \rightarrow 0.5$ $C_s'(6,7): 1 \rightarrow 2$		$C_s(3,4): 0.6 \rightarrow 0.4$ $C_s(4,5): 0.6 \rightarrow 0.9$ $C_g(3,0): 0.933 \rightarrow 1.033$ $C_g(4,0): 0.933 \rightarrow 0.883$	
B3	97.93 218.97 324.7	38.9 138.9 240.9 345.2	98.37 218.18 325.82 403.90 464.98	38.98 138.73 238.98 342.13 405.72 467.67

	$C_s'(5,6): 1 \rightarrow 0.5$ $C_s'(6,7): 1 \rightarrow 2$ $C_g'(6,0): 0.56 \rightarrow 1.06$		$C_s(3,4): 0.6 \rightarrow 0.4$ $C_s(4,5): 0.6 \rightarrow 0.9$ $C_g(3,0): 0.933 \rightarrow 1.033$ $C_g(4,0): 0.933 \rightarrow 1.233$ $C_g(5,0): 0.933 \rightarrow 1.033$	
C1	110 224.9	38.8 141 245.3	109.51 224.81 341.17 410.02 479.10	39.01 140.16 244.03 349.73 413.11 479.81
	$C_g'(1,0): 0.28 \rightarrow 0.56$ $C_g'(6,0): 0.56 \rightarrow 0.28$		$C_g(1,0): 0.467 \rightarrow 0.73$ $C_g(4,0): 0.933 \rightarrow 0.69$	
N o t e: (i) All capacitances are expressed in nF, (ii) A → B implies a change from A to B.				

Changes pertaining to the taps of the winding are found as a change in corresponding nodes of winding model. Figure 3.3 shows mapping of taps in the winding to nodes in the winding model.

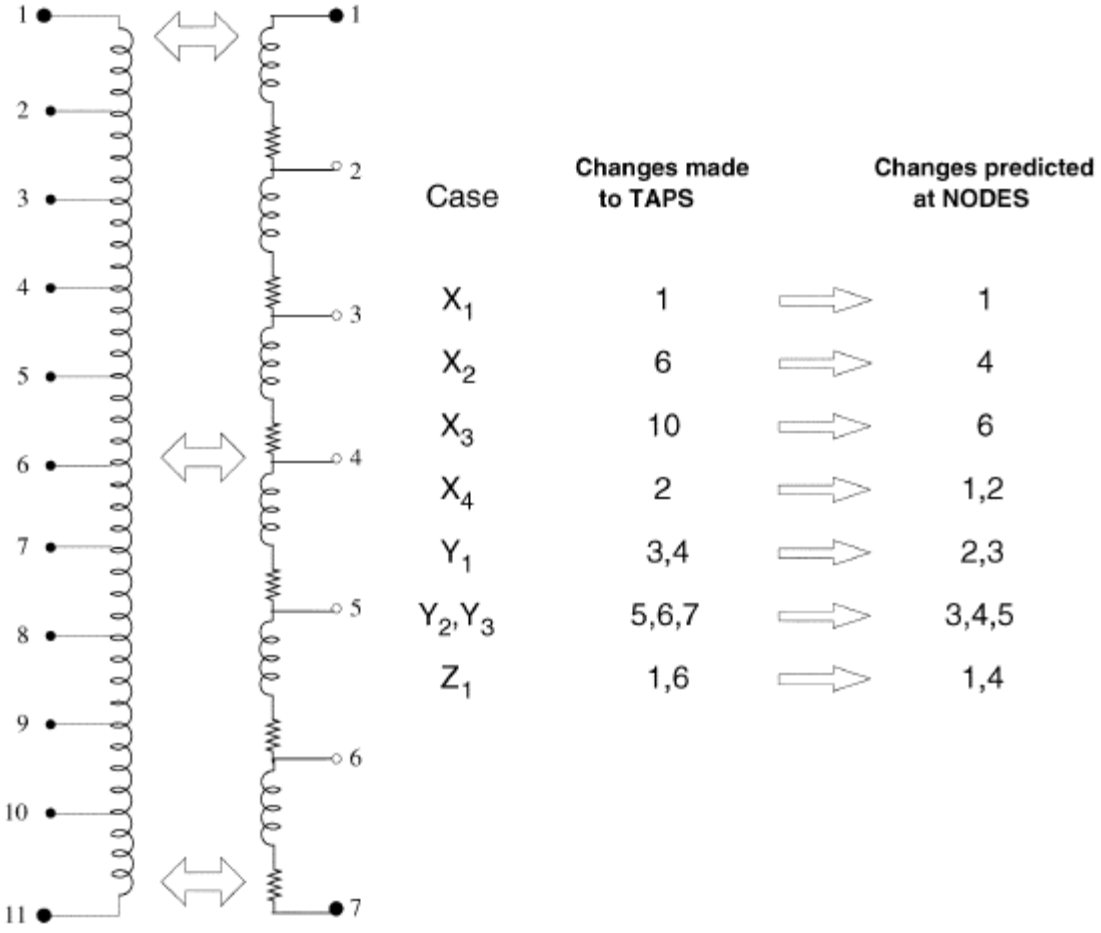

Figure 3.3 – Mapping of taps in the winding to nodes in the winding model (Cs and Cg exist, but are not shown)

Each of the cases is simulated and discussed in the next chapter.

3.4 Summary

State space approach is found to be suitable in model representation, since it can be easily constructed from the calculated parameters of the equivalent circuit. After getting correct state space model of the winding, it becomes possible to get transfer function. The path from state space model to TF is explained, and importance of diagonalization of system matrix A is presented as well. From obtained transfer function it is easy to get poles and zeros. Obtained State space model is shown in Appendix B and Appendix C in more detail. Appendix … represents transfer function of the system, poles and zeros.

Synthesized reference circuit is represented in discrete nodes. It allows to identify the location and extension of the winding damage. Capacitive changes pertained to the taps of the real winding are correctly mapped to the corresponding nodes of the equivalent circuit. Modeling of equivalent circuit in Matlab/Simulink allows to analyze the changes from the plots which is result of frequency response. Several cases is conducted to sure the correctness of mapping. After introducing changes measured frequencies of transformer winding and estimated frequencies of winding model are noted as in Table 3.1. Cases of changes are discussed in experimental chapter in more detail.

4 Experimental work on FRA methods

4.1 Winding model constructed using Simulink

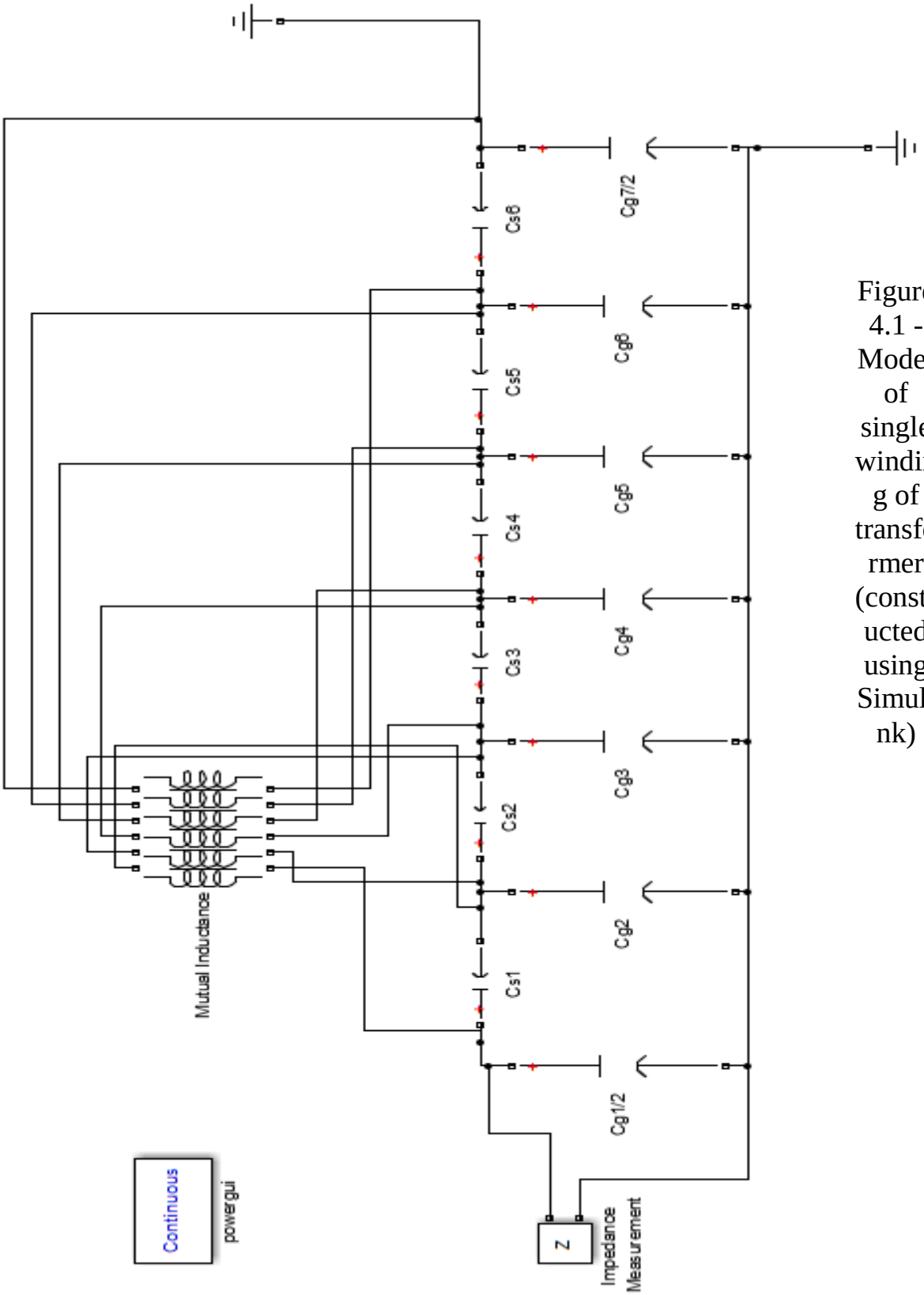

Figure 4.1 - Model of single winding of transformer (constructed using Simulink)

SimPowerSystems block of Simulink library is used to construct the model shown in Figure 4.1

Elements used in the model:

- mutual Inductance. Self and mutual inductances of each section where inputted. Resistance of each section is represented in matrix form. Figure 4.2 shows block diagram of mutual inductance.

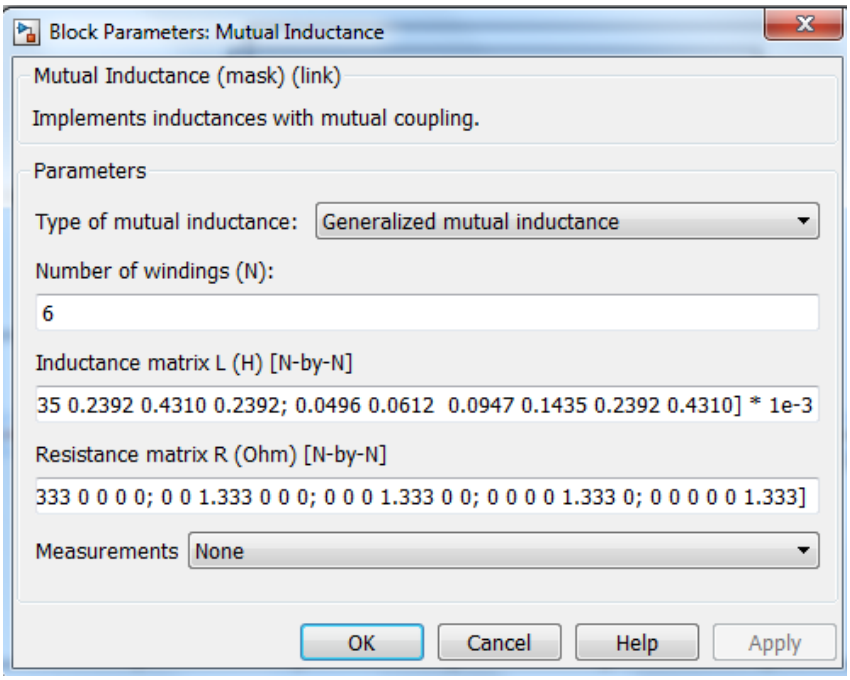

Figure 4.2 – Mutual inductance block parameters

- series RLC branch - as a branch type capacitance C is chosen. Since it is connect in series in the circuit, series RLC branch where chosen instead of parallel branch (refer to Figure 4.3).

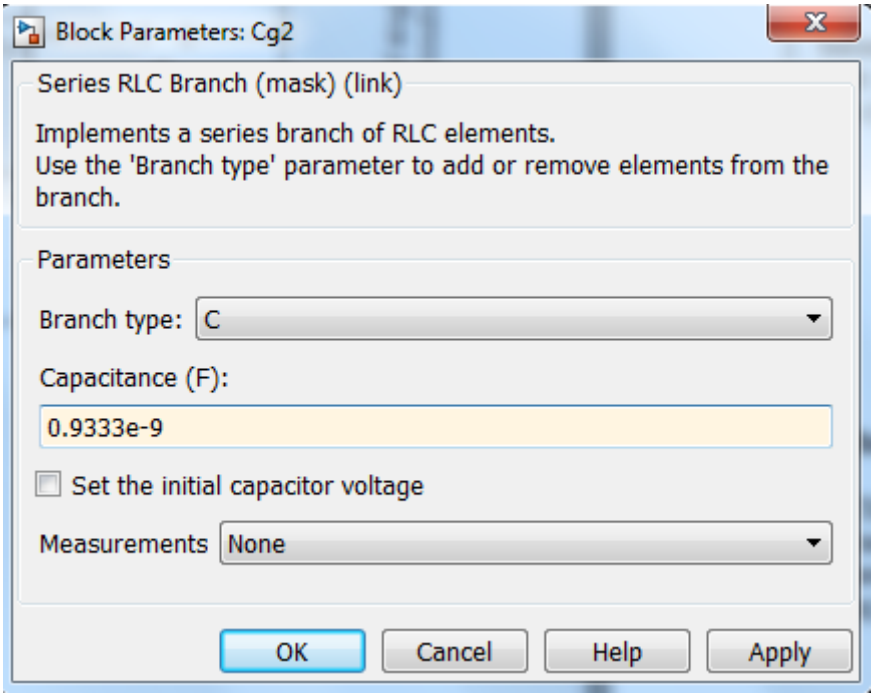

Figure 4.3 – Series RLC branch (branch type C)

- impedance measurement. The Impedance Measurement block measures the impedance between two nodes of a linear circuit as a function of the frequency. It consists of a current source Iz, connected between inputs one and two of the Impedance Measurement block, and a voltage measurement Vz, connected across the terminals of the current source. The network impedance is calculated as the transfer function H(s) from the current input to the voltage output of the state-space model.

$$H(s) = \frac{V_z(s)}{I_z(s)} \tag{4.1}$$

- powergui. The impedance (magnitude and phase) as function of frequency is displayed by using the Impedance vs Frequency Measurement tool of the Powergui block (Figure 4.4).

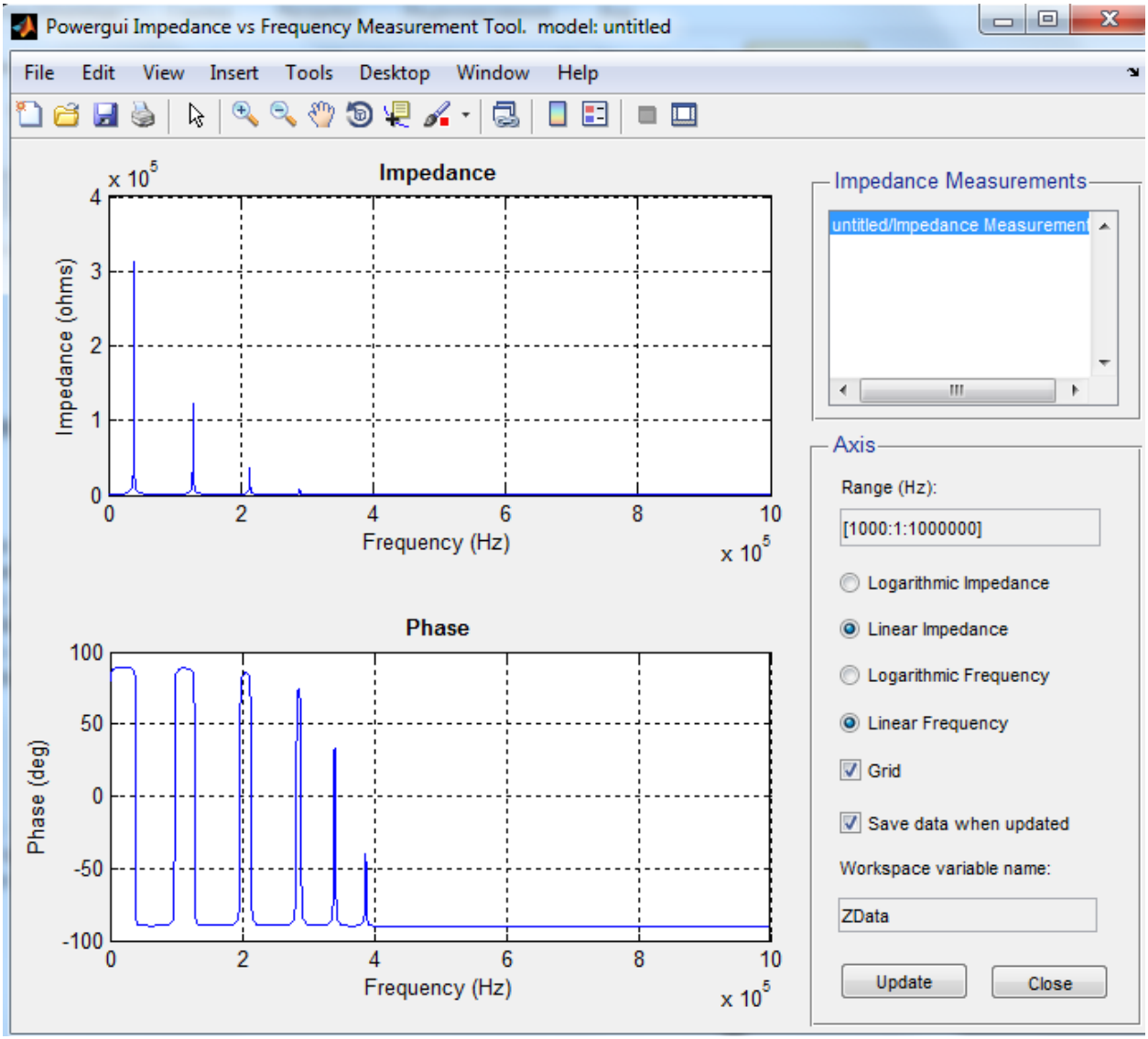

Figure 4.4 – Frequency response displayed by the Impedance vs Frequency Measurement tool of the Powergui block

4.2 Influence of space factor for winding frequency characteristics

The circuit representation comprising of series capacitance (Cs), shunt capacitance (Cg), self-inductance (Ls), lumped resistance (r), and mutual inductances (Mi-j) is known to adequately describe behavior of the transformer winding. Additionally in such representation the value of any element can be varied. Further, this representation permits analytical investigation, frequency-domain responses using circuit simulation software (Matlab). The self and mutual inductance values shown in Table 4.1. These values have been used during simulation studies.

Table 4.1 – Self and mutual inductances (Ls, Mi-j in mH)

Ls	M_{1-2}	M_{1-3}	M_{1-4}	M_{1-5}	M_{1-6}
0.4310	0.2392	0.1435	0.0947	0.0612	0.0496

Applicability of proposed method was initially verified by simulation studies on a 6-section circuit (as in Figure 3.1), details of which are given below:

- total Cg was chosen as 6nF and Cs as 1nF;
- ls and Mi-j corresponding to Table 4.1;
- a resistance (r) of 1.3333 Ω per section was used.

Different structures and capacities of transformer have different Cs and Cg; commonly it is defined by space factor.

$$\alpha = \sqrt{\frac{C_g}{C_s}} \tag{4.2}$$

Simulation results are discussed to study the influence of different space factor for winding frequency characteristic.

If changes in space factor there change in capacitive component of winding therefore shift in frequency characteristic of winding to indicate winding deformation. For simulation purpose α varies from 3 to 12.Winding frequency characteristics shown in Figure 4.5 for three different cases as α=3, α=7, α=12.

Figure 4.5 represents shift in frequency characteristic of winding when shunt capacitance Cg is constant as axial displacement. It shows increase in α resonant frequency of winding shift right side.

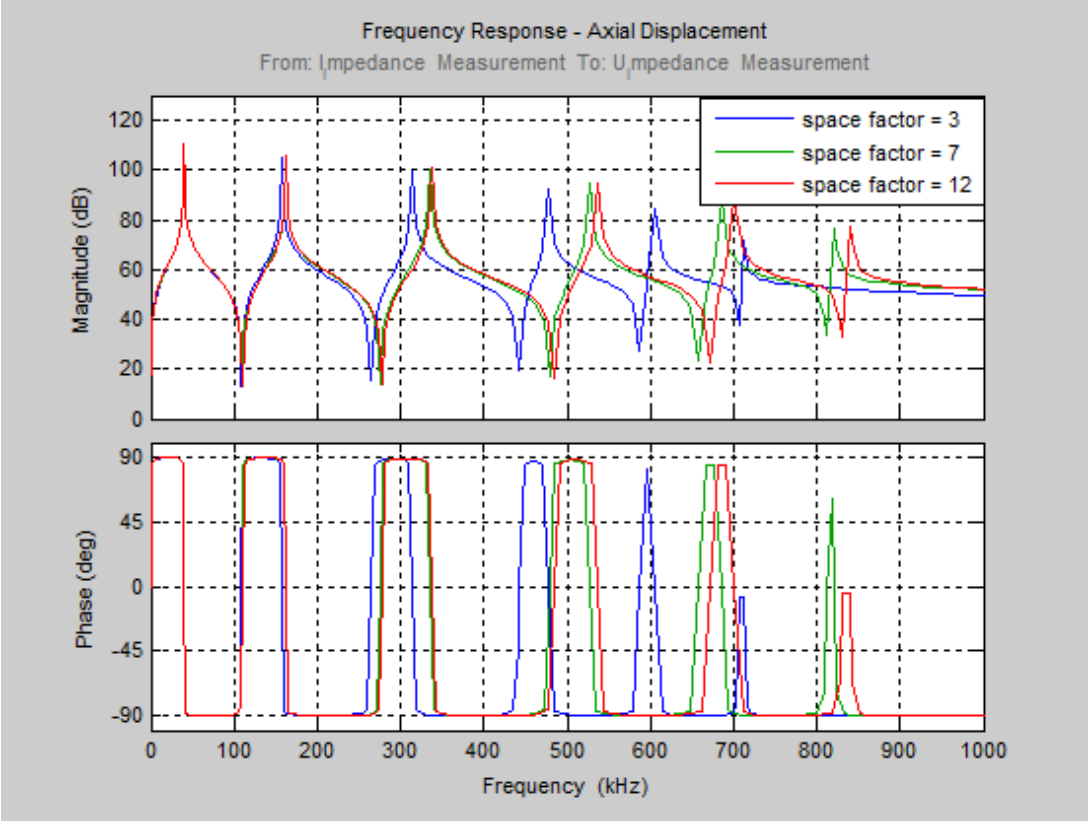

Figure 4.5 – Simulated FRA of uniform transformer winding (Cg is constant as axial displacement)

Similarly Figure 4.6.for three different cases as α=3, α=7, α=12. Figure 4.2 represents shift in frequency characteristic of winding when series capacitance Cs is constant as radial deformation. It shows increase in α resonant frequency of winding shift left side.

Comparing Figure 4.5 and Figure 4.6, in case axial deformation, when α increases band width of resonant frequency is much wider. Similarly in case axial deformation, when α increases band width of resonant frequency less.

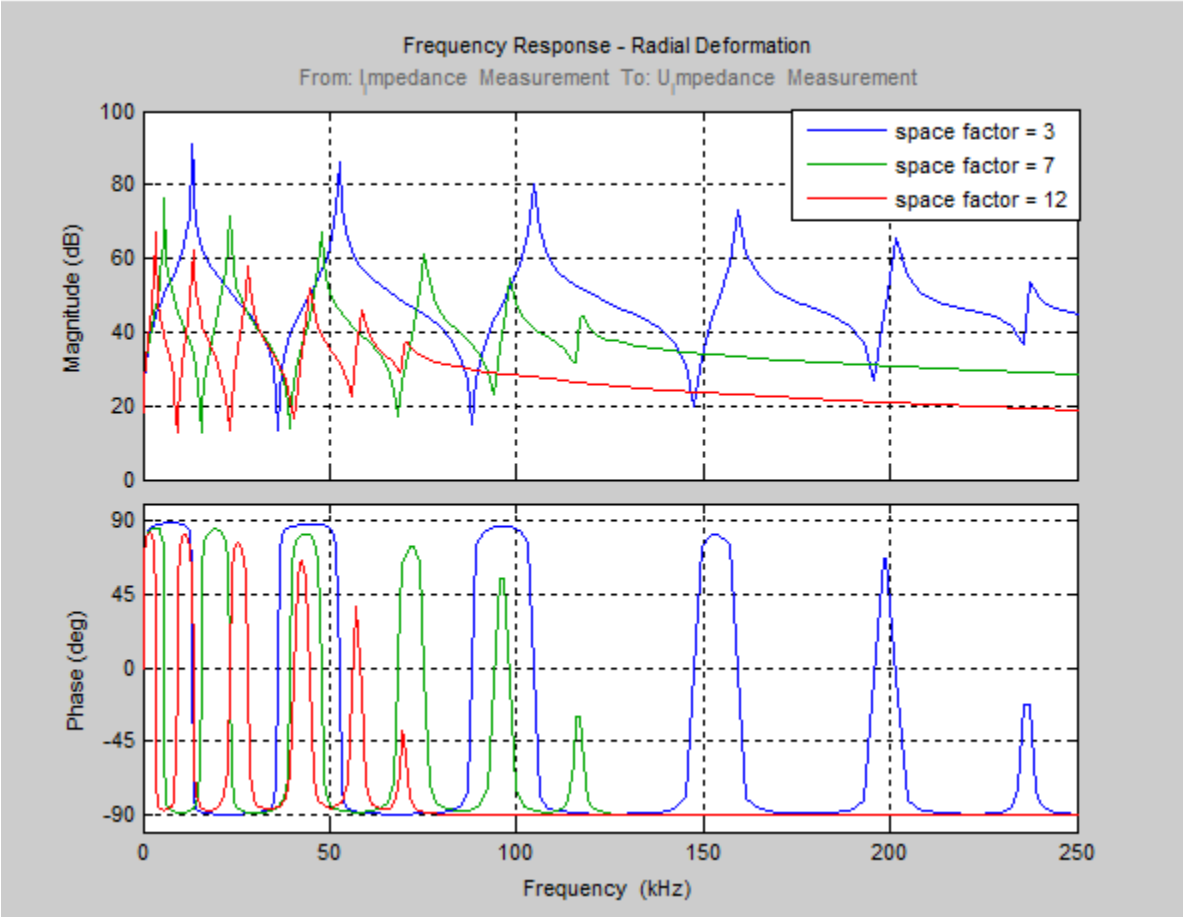

Figure 4.6 – Simulated FRA on uniform transformer winding (Cs is constant as radial deformation)

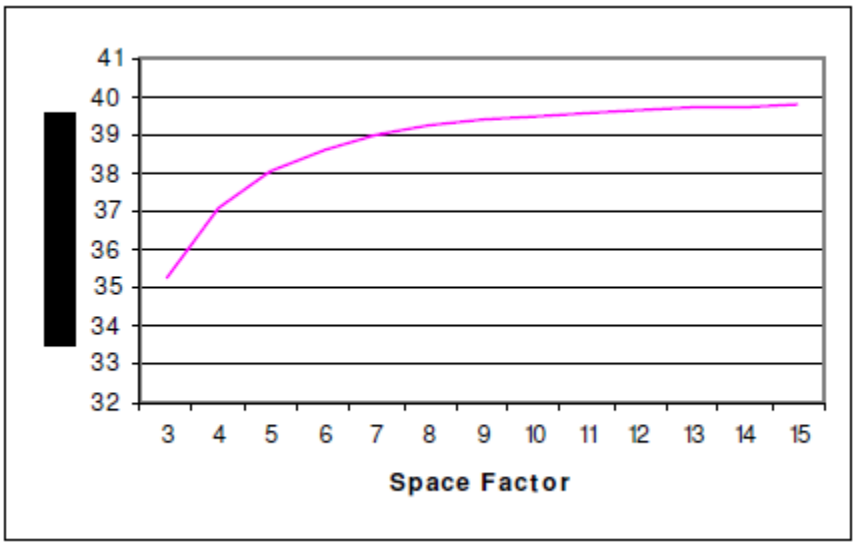

Figure 4.7 - Change in intact frequency w.r.t to space factor of transformer winding (axial displacement)

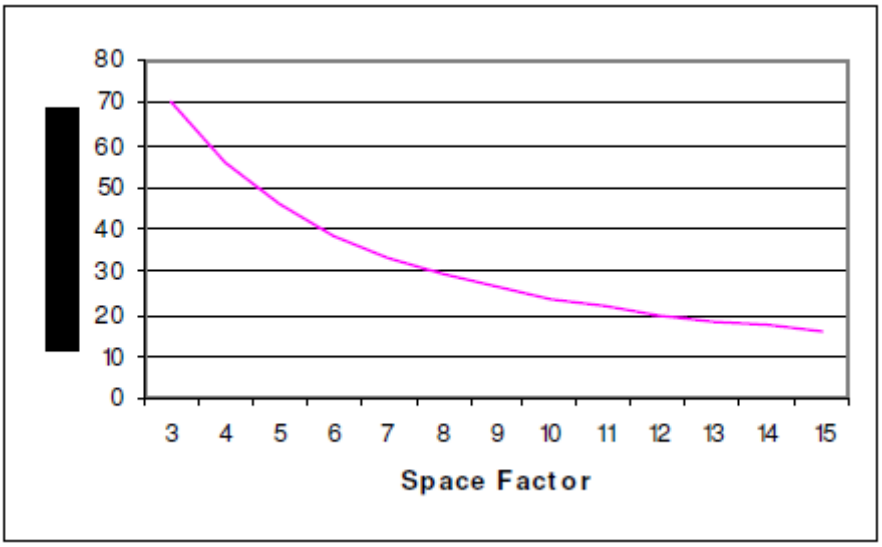

Figure 4.8 - Change in intact frequency w.r.t to space factor of transformer winding (radial deformation)

For Figure 4.7 and Figure 4.8 simulation studies are reported, frequency characteristic examined at first resonance frequency is called intact frequency of transformer. In Figure 4.7, when $\alpha < 9$ shift in intact frequency is gradually changes but $\alpha > 9$ shift in intact frequency is almost constant. But in Figure 4.8, $\alpha > 9$ shift in intact frequency is rapidly changes.

4.3 Introducing capacitive changes to continuous disk model winding

4.3.1 Changes pertaining to one node

In this group, changes are introduced in the model winding at a single node (which can occur at any position along the winding), namely A1 is at the line end, A2 is at the middle, A3 and A4 are close to the neutral end and line end, respectively.

As reference or primary data following parameters are used:

1. Cg was chosen as 0.933nF and Cs as 0.6nF;
2. Ls and Mi-j corresponding to Table 4.1;
3. A resistance (r) of 1.3333 Ω per section was used.

List of case studies:

a) Case A1. Here the shunt capacitance at the line end is increased from the reference value of 0.467 mH to 0.65 mH. The poles and zeros of transfer function (after changes are made) fixed and are represented in Table 3.1.

Figure 4.9 represents difference in the frequency characteristics between the model pertained to the change and primary (reference) model.

Table 4.2 shows poles and zeros of TF obtained from modified model.

Table 4.2 – Poles and zeros of transfer function

Poles	Zeros
$p_i = \delta_i \pm jw_i$ (in 1e+06)	$z_i = \tau_i \pm j\psi_i$ (in 1e+06)
-0.0050 ± 2.9749i	-0.0050± 2.9684i
-0.0040 ± 2.5977i	-0.0040 ± 2.5768i
-0.0031 ± 2.1615i	-0.0032 ± 2.1015i
-0.0020 ±1.5406i	-0.0021 ± 1.4125i
-0.0012 ± 0.8692i	-0.0012 ± 0.6610i
-0.0006 ±0.2451i	

Converting this values of poles and zeros to the scnf and ocnf respectively, as following:

From

$$w_i = \sqrt{w_{0,i}^2 - \delta_i^2} \tag{4.3}$$

$w_{o,i} = \sqrt{2.9749^2 + 0.0050^2} = 2.974904$

$f_{pi} = w_{o,i} \div 2 \div \pi = \ 0.473485 \approx 0.47349$

Putting it to the correct form we get $f_{pi} = 473.49$ kHz

We get values of scnf and ocnf corresponding to the Table 3.1 of the CaseA1;

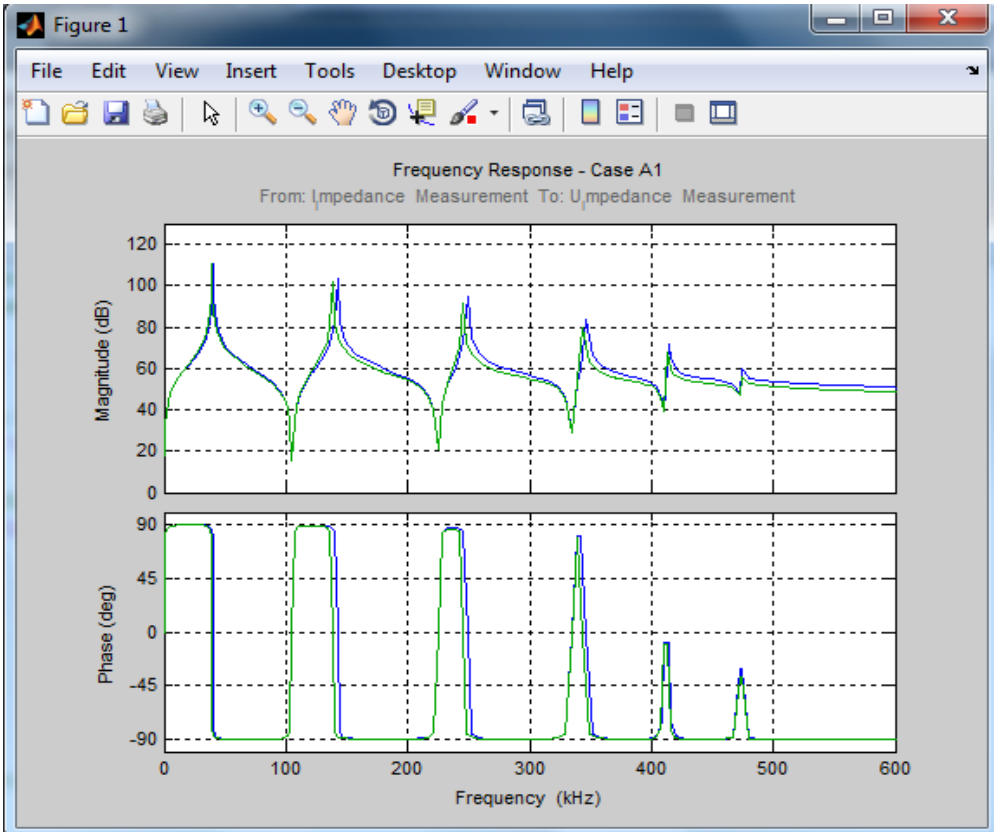

Figure 4.9 – Simulated FRA after Cg1 have changed

b) Case A2. In Case A2, the shunt capacitance at the middle (i.e.,TAP 6) of the winding was increased from 0.56 nF to 1.06 nF and it gets reflected as an increase of the shunt capacitance at the middle node (i.e., NODE 4) in the synthesized circuit from 0.933 nF to 1.35 nF.

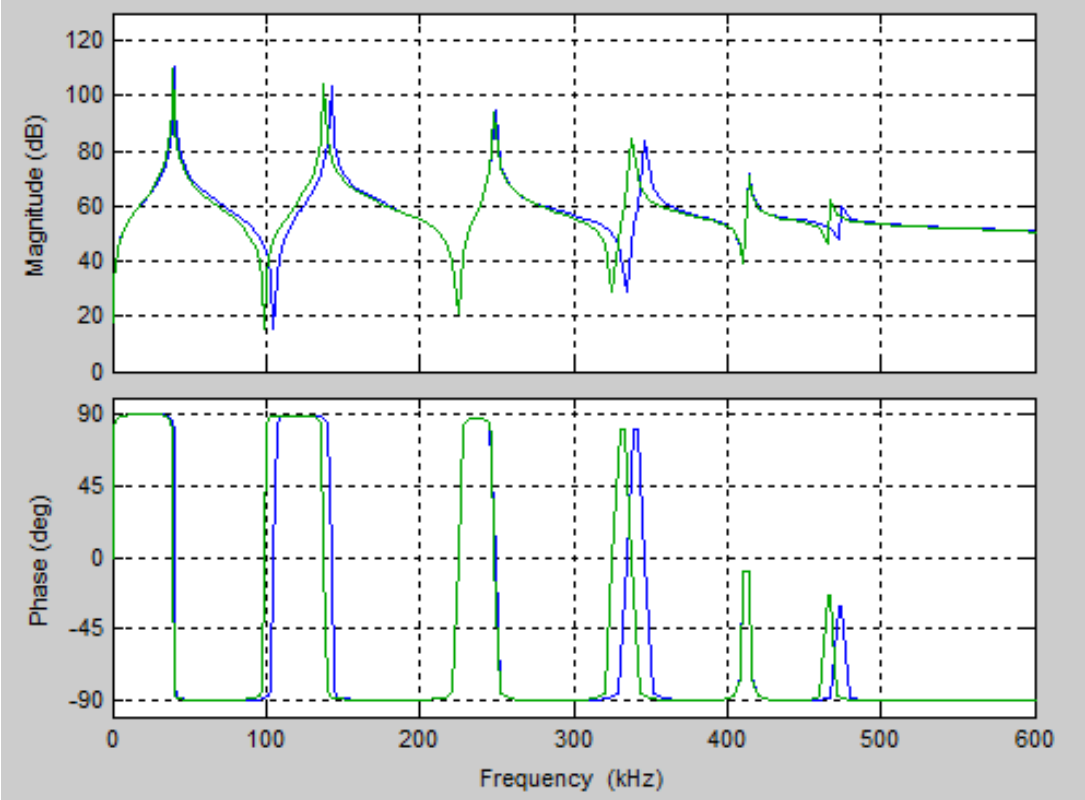

Figure 4.10 – Simulated FRA after Cg4 have changed

Rightward shift in the node 4 is noticeable from the bode plot, since the change have been exactly applied to the 4th section of the equivalent circuit;

c) Case A3 and Case A4. In Case A3, the shunt capacitance close to the neutral end (i.e., TAP 10) of the winding decreased from 0.56 nF to 0.1 nF and this was identified as a decrease

in the value of the shunt capacitance close to the neutral end (i.e., NODE 6) in the synthesized circuit from 0.933 nF to 0.67 nF. In cases and , it was observed that a discrete change introduced in the model winding is mapped to a discrete node in the synthesized circuit.

In Case A4, although only the shunt capacitance at TAP 2 alone is changed (in the model winding), the change gets reflected at two nodes (1 and 2) in the synthesized circuit and the reason for this will be explained later.

Simulated Frequency responses of the Case A3 and Case A4 are presented in Figure 4.11.

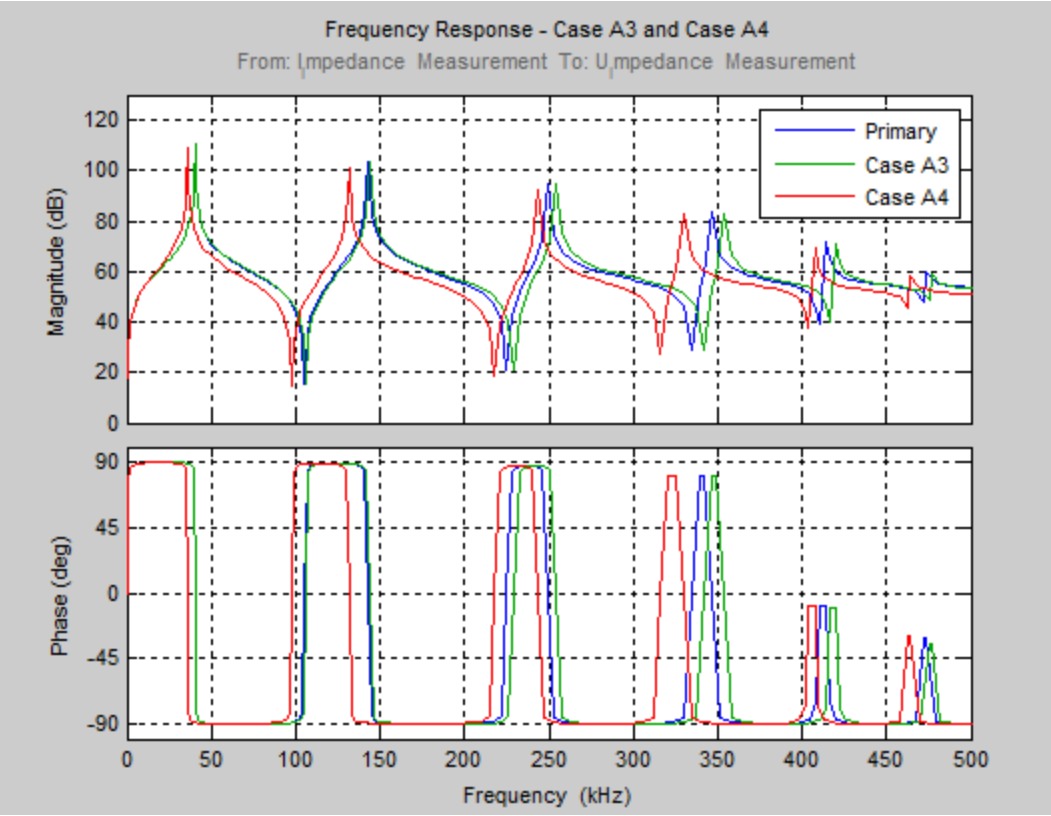

Figure 4.11 – FRA simulation for Case A3 and Case A4

There is a bigger difference in Case A4 comparing to Case A3, since changes have been pertained to the two nodes (Node 1 and 2) in Case A4 and the value of only one node (Node 1) has been changed.

4.3.2 Changes pertaining to more than one node

List of case studies:

a) Case B1, B2 and B3. In these cases the introduced changes pertained to more than one node of the model winding. In Case B1, series capacitance between Node 3 and 4 decreased from 0.6 nF to 0.5 nF and simultaneously, the shunt capacitance at Node 3 increased from 0.933 nF to 1.283 nF, and Node 2 decreased from 0.933 nF to 0.883 nF.

In Case B2, series capacitance between Node 3 and 4, also series capacitance between Node 4 and 5 were simultaneously decreased and increased from the reference value (that is, 0.6 nF) to 0.4 nF and 0.9 nF, respectively. Shunt capacitances of Nodes 3, 4 and 5 were increased from reference value 0.933 nF to 1.233 nF, 1.033 nF and 1.033 nF, respectively.

It was desirable to study the combined effect of two different cases. For this purpose, in Case B3, all of the changes corresponding to Cases A2 and B2 and were simultaneously introduced in the model winding (see Table 3.1).

Figure 4.12 shows corresponding frequency responses for Case B1.

Figure 4.13 shows corresponding frequency responses for Case B2.

Figure 4.14 shows corresponding frequency responses for Case B3, which has a combined effect of two different cases, viz. Case A2 and Case B2.

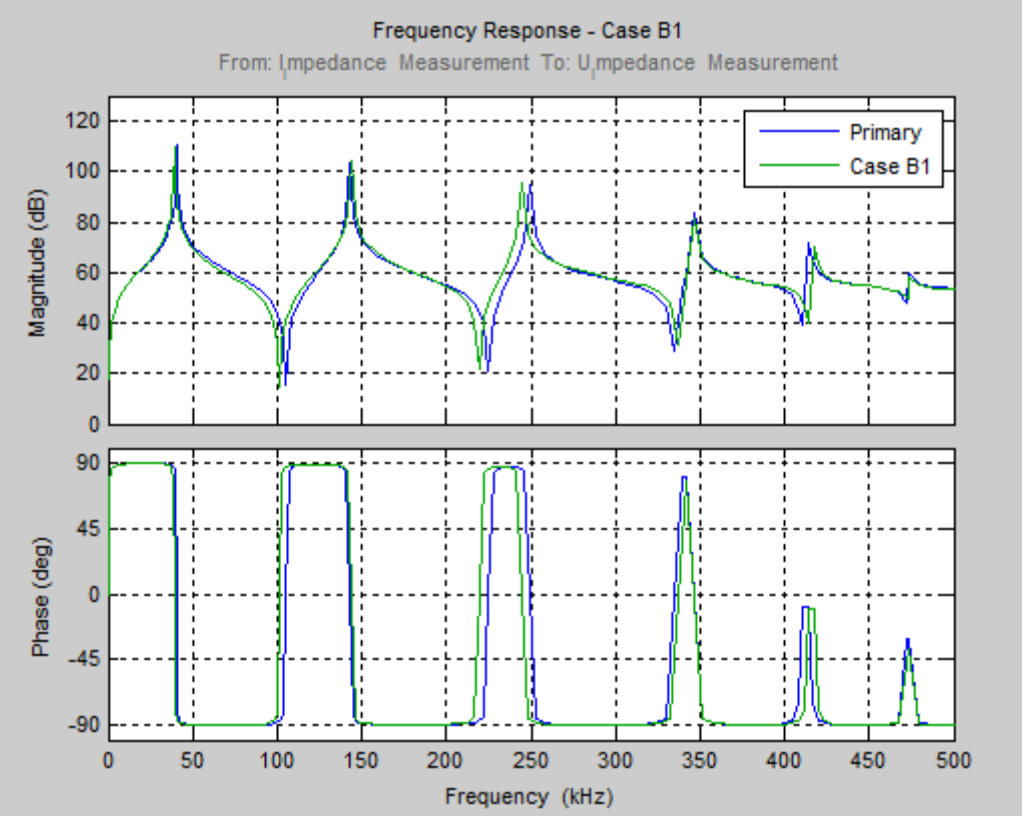

Figure 4.12 – FRA simulation for Case B1

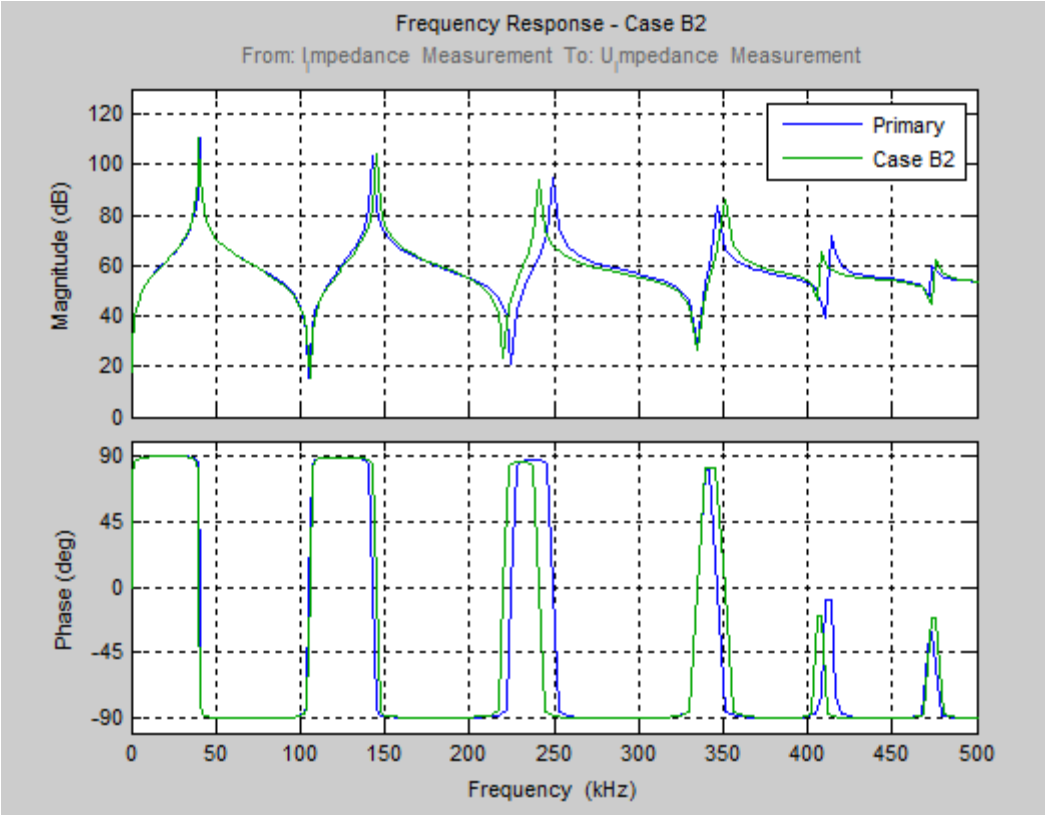

Figure 4.13 – FRA simulation for Case B2

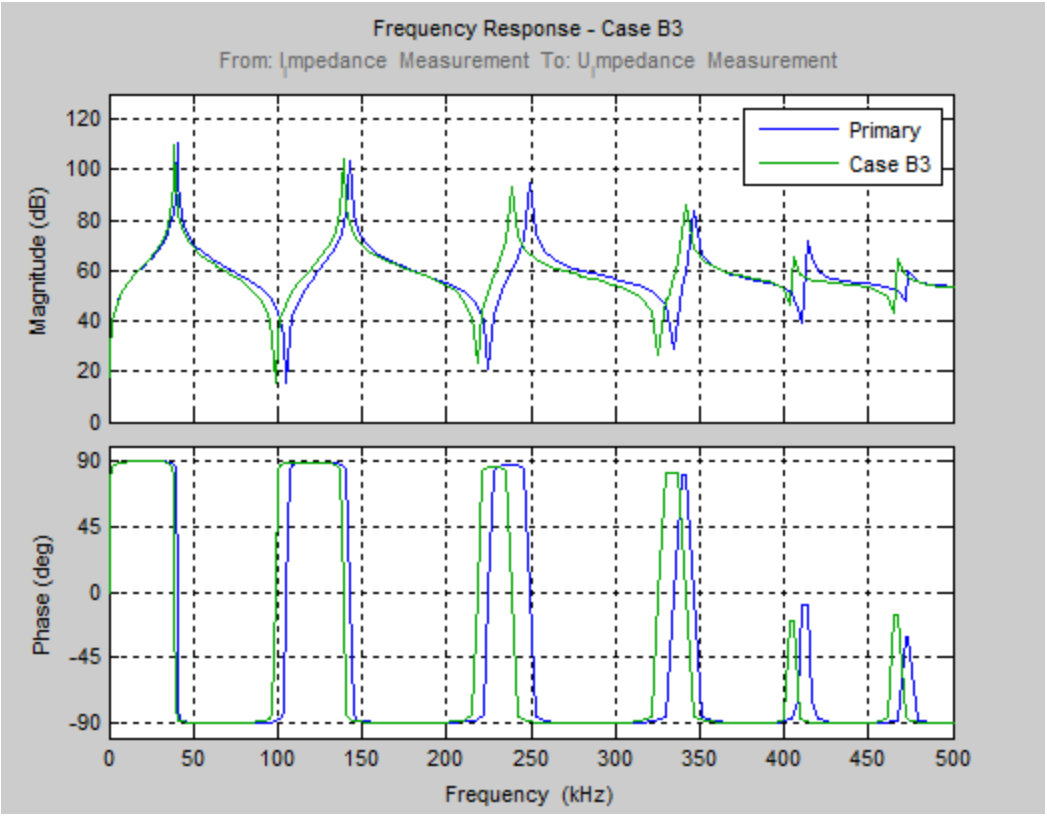

Figure 4.14 – FRA Simulation for Case B3

4.3.3 Changes to physically separated nodes

In reality, mechanical deformations often result in damages that affect different parts of the winding. Hence, it is interesting to simulate such a situation to the extent possible. With this in mind, in Case C1, capacitances at Node 1 (line end) and 4 (middle) were simultaneously increased and decreased, respectively, by the same margin. Increase of shunt capacitance in Node 1 from 0.467 nF to 0.73 nF, and decrease of shunt capacitance of Node 4 from 0.933 nF to 0.69 nF effects the frequency response. Comparison between frequency response of reference model and the model pertained to the change is presented and difference in frequency ranges can be obviously seen from Figure 4.15.

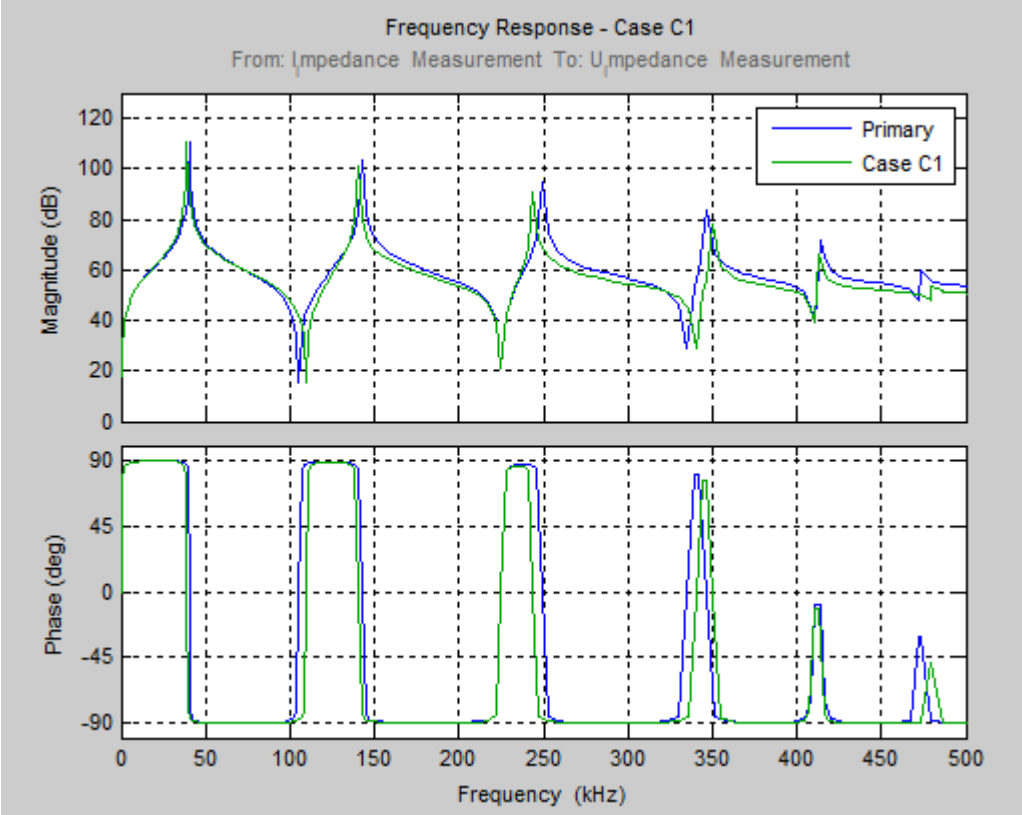

Figure 4.15 – FRA Simulation for Case C1

As a product of these case studies, the results can be summarized as follows:

- the frequency response analysis are obtained using the power_analyze and bodeplot for the impedance measurement whereas the transfer function are obtained using power_analyze, ss2tf, tf and bodeplot all from the MATLAB command Signal Processing Toolbox. The function of power_analyze computes the equivalent state-space model of the specified electrical model built within SimpowerSystems software. Also the ss2tf converts state space filter parameters to transfer function form whereas tf command creates transfer function model. Finally the bodeplot function graphs the magnitude and phase of the dynamic system [28];

- the phase response was also considered, although magnitude response for the diagnosis analysis was the main parameter. If phase response is utilized it must be correctly represented. When the phase is shown from -90 to +90 ($-\pi/2$ and $\pi/2$ rad) there are some jumps when the angle exceeds one of the limits. An algorithm that wraps the phase was used as a wrap function (MATLAB's Signal Process Toolbox) [28];

- capacitive changes pertained to the model winding, effects frequency response by changing the frequency range, by changing the transfer function poles and zeros (scnfs and ocnfs of equivalent ciruit). If changes have done on several nodes of the model, then the frequency response in respect to the reference (primary) frequency response, will differ more comparing with the change made to the single node;

- only changing shunt capacitance and remaining series capacitance constant leads to the leftward shift of the winding frequency. It is the case of radial deformation;

- only changing series capacitance and remaining shunt capacitance constant leads to the rightward shift of the winding frequency. It is the case of axial displacement.

Conclusion

In the present work, experimental and theoretical studies of power transformer winding frequency characteristics are fulfilled. Main practical and scientific results of the dissertation work are as follows:

- the healthy and deformed cases are analyzed by comparative approach on model winding using Simulink software tool;
- simulation model of the winding corresponding to the synthesized equivalent circuit, and FRA is simulated by pertaining capacitive changes to the model in Matlab programming environment;
- mathematical model of transformer winding is constructed, and influence of winding parameters to the model is investigated; State equation of the system is considered;
- simulation studies of analysis of equivalent circuit of transformer winding are presented using state space approach. Conversion from the state space form to the transfer function (TF) form by diagonalizing system matrix is presented;
- algorithms of synthesizing equivalent circuit by iterative approach are described. Usage of these algorithms in winding damage localization is stated. Correspondence of faults between real winding and model of the winding in localization issues are discussed.

Reference

1. Forge Pleite, Carlos Gonzalez, Juan Vazquez, Antonio Lazaro, “Power transformer core fault diagnosis using frequency response analysis”, IEEE MELECON 2006, May 16-19, Benalmadena, Spain, pp 1126-1129
2. Electric Power Transformer Engineering/ edited by James H. Harlow
3. Transformer Engineering Design and Practice, S.V. Kulkarni
4. Выбор и эксплуатация силовых трансформаторов: Учебное пособие для Вузов/ Г.Ф. Быстрицкий , Б.И. Кудрин, - М: Издательский центр «Академия», 2003. – 176 с.
5. Актуальные проблемы энергетической отрасли Республики Казахстан, Журнал «Энергетика», №3(34) август 2010г. (http://www.kazenergy.kz/arhiv/34/6.htm)
6. CIGRE Working Group 05, “An International Survey on Failures in Large Power Transformers in Service”, Electra. No.88, May 1983.
7. Kogan, V.I., et al., "Failure Analysis of EHV Transformers", IEEE Transactions on Power Delivery. Vol. 3, No. 2, pp. 672-683, April 1988.
8. www.eum.kz
9. РД 34.45-51.300-97. Объем и нормы испытаний электрооборудования / Под общ. ред. Б.А. Алексеева, Ф.Л. Когана, Л.Г. Мамиконянца. — 6-е изд., с изм. и доп.- М.: Изд-во НЦ ЭНАС, 2001.-256 с.
10. Lech, W. and Tyminski, L. Detecting transformer winding damage by the Low Voltage Impulse method. Electrical Review, No. 21, Vol 179, November 1966, pp 768-772.
11. E.P. Dick, C.C. Erven, Transformer diagnostic testing by frequency response analysis, IEEE Trans. Power Appar. Syst. PAS-97 (November/December) (1978) 2144–2153.
12. K. Ragavan, L. Satish, Localization of changes in a model winding based on terminal measurements: experimental study, IEEE Trans. Power Deliv. 22 (July) (2007) 1557–1565.
13. E. Rahimpour, J. Christian, K. Feser, H. Moheseni, Transfer function method to diagnose axial displacement and radial deformation of transformer windings, IEEE Trans. Power Deliv. 18 (April) (2003) 493–505.
14. S.A. Ryder, Diagnosing transformer faults using frequency response analysis, IEEE EI Mag. 19 (March–April (2)) (2003) 16–22.
15. M. Florkowski, J. Furgal, Detection of transformer winding deformations based on the transfer function measurements and simulations, J. Meas. Sci. Technol. 14 (2003) 1986–1992.
16. Дробышевский А.А., Левицкая Е.И. Индикация повреждений обмоток трансформаторов с использованием метода низковольтных импульсов // Электротехника, 1994, №10, с. 27-28.
17. Th.Aschwanden, M.Hassig, J.Fuhr, O.Lorin, V.Der Hoahanessian, W.Zaengl, A.Schenk, P.Zwelaclcer, A.Piras, J.Dutoit. Development and application of new

condition assessment methods for powerr transformers // Сессия CIGRE-98, доклад № 12-07.
18. Eiji Ozaki, Shinya Soyama. An Application of FRA to fault Location on transformer // Hamakowaswku operation, Power system, Toshibo Corp. Kawasakum, Japan.
19. Fred Fetherston. Some sensitivity issues for FRA measurement // Sympo¬sium CIGRE, 2001, Cairus, Australia.
20. F. de Leon and A. Semlyen, “Efficient calculation of elementary parameters of transformers,” IEEE Trans. Power Del., vol. 7, no. 1, pp. 376–383, Jan. 1992.
21. T. Leibfried and K. Feser, “Monitoring of power transformers using the transfer function method,” IEEE Trans. Power Del., vol. 14, no. 4, pp. 1333–1341, Oct. 1999.
22. E. A. Guillemin, Theory of Linear Physical Systems. NewYork:Wiley, 1963.
23. E. A. Guillemin, The Mathematics of Circuit Analysis. New York: Wiley, 1951.
24. E. A. Guillemin, Synthesis of Passive Networks. New York: Wiley, 1962.
25. Ragavan, K. & Satish, L. (2007). Localization of Changes in a Model Winding based on Terminal Measurements: Experimental Study. IEEE Trans. Power Delivery, vol. 22, no. 3, July 2007, pp. 1557-1565.
26. P. A. Abetti and F. J. Maginniss, “Natural frequencies of coils and windings determined by equivalent circuit,” AIEE Trans., vol. 72, pt. III, pp. 495–504, Jun. 1953.
27. L. Satish and A. Jain, “Structure of transfer function of transformers with special reference to interleaved windings,” IEEE Trans. Power Del., vol. 17, no. 3, pp. 754–760, Jul. 2002.
28. MATLAB, Ver. 2013. "8.1.0.604 (R2013a), The MathWorks." *Inc., Natick, MA*.

Appendix A. Winding parameter calculation

Inductance matrix calculation

Inductance matrix is n by n matrix, where n = 6 to the number of the sections of the ladder network.

Inductance values shown in Table 4.1 are represented in [L] matrix form (Ls, Mi-j in mH) as following:

$$[L] = \begin{bmatrix} Ls_1 & M_{1-2} & M_{1-3} & M_{1-4} & M_{1-5} & M_{1-6} \\ M_{1-2} & Ls_2 & M_{1-2} & M_{1-3} & M_{1-4} & M_{1-5} \\ M_{1-3} & M_{1-2} & Ls_3 & M_{1-2} & M_{1-3} & M_{1-4} \\ M_{1-4} & M_{1-3} & M_{1-2} & Ls_4 & M_{1-2} & M_{1-3} \\ M_{1-5} & M_{1-4} & M_{1-3} & M_{1-2} & Ls_5 & M_{1-2} \\ M_{1-6} & M_{1-5} & M_{1-4} & M_{1-3} & M_{1-2} & Ls_6 \end{bmatrix} =$$

$$\begin{bmatrix} 0.4310 & 0.2392 & 0.1435 & 0.0947 & 0.0612 & 0.0496 \\ 0.2392 & 0.4310 & 0.2392 & 0.1435 & 0.0947 & 0.0612 \\ 0.1435 & 0.2392 & 0.4310 & 0.2392 & 0.1435 & 0.0947 \\ 0.0947 & 0.1435 & 0.2392 & 0.4310 & 0.2392 & 0.1435 \\ 0.0612 & 0.0947 & 0.1435 & 0.2392 & 0.4310 & 0.2392 \\ 0.0496 & 0.0612 & 0.0947 & 0.1435 & 0.2392 & 0.4310 \end{bmatrix}, \quad \text{(A.1)}$$

where $Ls_1 = Ls_2 = \cdots = Ls_6$

Nodal capacitance matrix calculation

Nodal capacitance matrix [K] (Cs, Cg in nF) is constructed as per (A.2):

$$\begin{bmatrix} Cs + Cg_1/2 & -Cs & 0 & 0 & 0 & 0 \\ -Cs & 2Cs + Cg_2 & -Cs & 0 & 0 & 0 \\ 0 & -Cs & 2Cs + Cg_3 & -Cs & 0 & 0 \\ 0 & 0 & -Cs & 2Cs + Cg_4 & -Cs & 0 \\ 0 & 0 & 0 & -Cs & 2Cs + Cg_5 & -Cs \\ 0 & 0 & 0 & 0 & -Cs & 2Cs + Cg_6 \end{bmatrix}$$

$$[K] = \begin{bmatrix} 1.5 & -1 & 0 & 0 & 0 & 0 \\ -1 & 3 & -1 & 0 & 0 & 0 \\ 0 & -1 & 3 & -1 & 0 & 0 \\ 0 & 0 & -1 & 3 & -1 & 0 \\ 0 & 0 & 0 & -1 & 3 & -1 \\ 0 & 0 & 0 & 0 & -1 & 3 \end{bmatrix}, \quad \text{(A.2)}$$

where $Cg_1 = Cg_2 = \cdots = Cg_6$

Diagonal Resistance matrix representation

[R] is a diagonal matrix, where r = 1.333 Ω

$$[R] = \begin{bmatrix} 1.3333 & 0 & 0 & 0 & 0 & 0 \\ 0 & 1.3333 & 0 & 0 & 0 & 0 \\ 0 & 0 & 1.3333 & 0 & 0 & 0 \\ 0 & 0 & 0 & 1.3333 & 0 & 0 \\ 0 & 0 & 0 & 0 & 1.3333 & 0 \\ 0 & 0 & 0 & 0 & 0 & 1.3333 \end{bmatrix} \quad \text{(A.3)}$$

Appendix B. State Model calculation

The A Matrix

Time-derivatives of nodes can be expressed as, assigning $[E_i] = -[K]^{-1}[T]$:

$$\begin{bmatrix} de_1/dt \\ de_2/dt \\ \vdots \\ de_n/dt \end{bmatrix} = [E_i] \begin{bmatrix} i_1 \\ i_2 \\ \vdots \\ i_n \end{bmatrix}, \tag{B.1}$$

$$[E_i] = -\begin{bmatrix} 1.5 & -1 & 0 & 0 & 0 & 0 \\ -1 & 3 & -1 & 0 & 0 & 0 \\ 0 & -1 & 3 & -1 & 0 & 0 \\ 0 & 0 & -1 & 3 & -1 & 0 \\ 0 & 0 & 0 & -1 & 3 & -1 \\ 0 & 0 & 0 & 0 & -1 & 3 \end{bmatrix}^{-1} \begin{bmatrix} 1 & 0 & \dots & 0 & 0 \\ -1 & 1 & \dots & 0 & 0 \\ \vdots & \vdots & \ddots & \vdots & \vdots \\ 0 & 0 & \dots & -1 & 1 \end{bmatrix} =$$

$$= \begin{bmatrix} -5.5280e+08 & -2.1118e+08 & -8.0745e+07 & -3.1056e+07 & -1.2422e+07 & -6.2112e+06 \\ 1.7081e+08 & -3.1677e+08 & -1.2112e+08 & -4.6584e+07 & -1.8634e+07 & -9.3168e+06 \\ 6.5217e+07 & 2.6087e+08 & -2.8261e+08 & -1.0870e+08 & -4.3478e+07 & -2.1739e+07 \\ 2.4845e+07 & 9.9379e+07 & 2.7329e+08 & -2.7950e+08 & -1.1180e+08 & -5.5901e+07 \\ 9.3168e+06 & 3.7267e+07 & 1.0248e+08 & 2.7019e+08 & -2.9193e+08 & -1.4596e+08 \\ 3.1056e+06 & 1.2422e+07 & 3.4161e+07 & 9.0062e+07 & 2.3602e+08 & -3.8199e+08 \end{bmatrix},$$

$$\begin{bmatrix} di_1/dt \\ di_2/dt \\ \vdots \\ di_n/dt \end{bmatrix} = [I_e] \begin{bmatrix} e_1 \\ e_2 \\ \vdots \\ e_n \end{bmatrix} + [I_i] \begin{bmatrix} i_1 \\ i_2 \\ \vdots \\ i_n \end{bmatrix}, \tag{B.2}$$

where $[I_e] = [L]^{-1}[T]^t$, *and* $[I_i] = -[L]^{-1}[R]$:

$$[I_e] = \begin{bmatrix} 0.4310 & 0.2392 & 0.1435 & 0.0947 & 0.0612 & 0.0496 \\ 0.2392 & 0.4310 & 0.2392 & 0.1435 & 0.0947 & 0.0612 \\ 0.1435 & 0.2392 & 0.4310 & 0.2392 & 0.1435 & 0.0947 \\ 0.0947 & 0.1435 & 0.2392 & 0.4310 & 0.2392 & 0.1435 \\ 0.0612 & 0.0947 & 0.1435 & 0.2392 & 0.4310 & 0.2392 \\ 0.0496 & 0.0612 & 0.0947 & 0.1435 & 0.2392 & 0.4310 \end{bmatrix}^{-1} \times 10^{-3} \times$$

$$\times \begin{bmatrix} 1 & 0 & \dots & 0 & 0 \\ -1 & 1 & \dots & 0 & 0 \\ \vdots & \vdots & \ddots & \vdots & \vdots \\ 0 & 0 & \dots & -1 & 1 \end{bmatrix}^t =$$

$$= \begin{bmatrix} 3.3647e+03 & -5.1607e+03 & 1.7347e+03 & -39.2101 & 158.8265 & -175.9405 \\ -1.7960e+03 & 6.1152e+03 & -6.0805e+03 & 1.7501e+03 & -122.6172 & 192.0980 \\ -61.2989 & -1.6999e+03 & 6.0806e+03 & -6.0770e+03 & 1.7465e+03 & -89.3458 \\ -100.5089 & 89.3458 & -1.7465e+03 & 6.0770e+03 & -6.0806e+03 & 1.6999e+03 \\ 58.3176 & -192.0980 & 122.6172 & -1.7501e+03 & 6.0805e+03 & -6.1152e+03 \\ -117.6229 & 175.9405 & -158.8265 & 39.2101 & -1.7347e+03 & 5.1607e+03 \end{bmatrix},$$

$$[I_i] = -\begin{bmatrix} 0.4310 & 0.2392 & 0.1435 & 0.0947 & 0.0612 & 0.0496 \\ 0.2392 & 0.4310 & 0.2392 & 0.1435 & 0.0947 & 0.0612 \\ 0.1435 & 0.2392 & 0.4310 & 0.2392 & 0.1435 & 0.0947 \\ 0.0947 & 0.1435 & 0.2392 & 0.4310 & 0.2392 & 0.1435 \\ 0.0612 & 0.0947 & 0.1435 & 0.2392 & 0.4310 & 0.2392 \\ 0.0496 & 0.0612 & 0.0947 & 0.1435 & 0.2392 & 0.4310 \end{bmatrix}^{-1} \times 10^{-3} \times$$

$$\times \begin{bmatrix} 1.3333 & 0 & 0 & 0 & 0 & 0 \\ 0 & 1.3333 & 0 & 0 & 0 & 0 \\ 0 & 0 & 1.3333 & 0 & 0 & 0 \\ 0 & 0 & 0 & 1.3333 & 0 & 0 \\ 0 & 0 & 0 & 0 & 1.3333 & 0 \\ 0 & 0 & 0 & 0 & 0 & 1.3333 \end{bmatrix} =$$

$$= \begin{bmatrix} -4.4851e+03 & 2.3941e+03 & 81.7114 & 133.9784 & -77.7374 & 156.7913 \\ 2.3941e+03 & -5.7575e+03 & 2.3477e+03 & 14.8805 & 178.3292 & -77.7374 \\ 81.7114 & 2.3477e+03 & -5.7577e+03 & 2.3430e+03 & 14.8805 & 133.9784 \\ 133.9784 & 14.8805 & 2.3430e+03 & -5.7577e+03 & 2.3477e+03 & 81.7114 \\ -77.7374 & 178.3292 & 14.8805 & 2.3477e+03 & -5.7575e+03 & 2.3941e+03 \\ 156.7913 & -77.7374 & 133.9784 & 81.7114 & 2.3941e+03 & -4.4851e+03 \end{bmatrix}$$

$$[A] = \begin{bmatrix} 0 & [E_i] \\ [I_e] & [I_i] \end{bmatrix} =$$

$$\begin{vmatrix} 0 & 0 & 0 & 0 & 0 & 0 \\ 0 & 0 & 0 & 0 & 0 & 0 \\ 0 & 0 & 0 & 0 & 0 & 0 \\ 0 & 0 & 0 & 0 & 0 & 0 \\ 0 & 0 & 0 & 0 & 0 & 0 \\ 0 & 0 & 0 & 0 & 0 & 0 \\ 3.3647e+03 & -5.1607e+03 & 1.7347e+03 & -39.2101 & 158.8265 & -175.9405 \\ -1.7960e+03 & 6.1152e+03 & -6.0805e+03 & 1.7501e+03 & -122.6172 & 192.0980 \\ -61.2989 & -1.6999e+03 & 6.0806e+03 & -6.0770e+03 & 1.7465e+03 & -89.3458 \\ -100.5089 & 89.3458 & -1.7465e+03 & 6.0770e+03 & -6.0806e+03 & 1.6999e+03 \\ 58.3176 & -192.0980 & 122.6172 & -1.7501e+03 & 6.0805e+03 & -6.1152e+03 \\ -117.6229 & 175.9405 & -158.8265 & 39.2101 & -1.7347e+03 & 5.1607e+03 \end{vmatrix}$$

$-5.5280e+08$	$-2.1118e+08$	$-8.0745e+07$	$-3.1056e+07$	$-1.2422e+07$	$-6.2112e+06$
$1.7081e+08$	$-3.1677e+08$	$-1.2112e+08$	$-4.6584e+07$	$-1.8634e+07$	$-9.3168e+06$
$6.5217e+07$	$2.6087e+08$	$-2.8261e+08$	$-1.0870e+08$	$-4.3478e+07$	$-2.1739e+07$
$2.4845e+07$	$9.9379e+07$	$2.7329e+08$	$-2.7950e+08$	$-1.1180e+08$	$-5.5901e+07$
$9.3168e+06$	$3.7267e+07$	$1.0248e+08$	$2.7019e+08$	$-2.9193e+08$	$-1.4596e+08$
$3.1056e+06$	$1.2422e+07$	$3.4161e+07$	$9.0062e+07$	$2.3602e+08$	$-3.8199e+08$

$-4.4851e+03$	$2.3941e+03$	81.7114	133.9784	-77.7374	156.7913
$2.3941e+03$	$-5.7575e+03$	$2.3477e+03$	14.8805	178.3292	-77.7374
81.7114	$2.3477e+03$	$-5.7577e+03$	$2.3430e+03$	14.8805	133.9784
133.9784	14.8805	$2.3430e+03$	$-5.7577e+03$	$2.3477e+03$	81.7114
-77.7374	178.3292	14.8805	$2.3477e+03$	$-5.7575e+03$	$2.3941e+03$
156.7913	-77.7374	133.9784	81.7114	$2.3941e+03$	$-4.4851e+03$

Appendix C. Matlab Code for State Model Formulation

```
% This code is generated to construct state model

% Parameter matrices [K], [R], [L] assignment
% [K] is 6x6 matrix with the values of nodal capacitance matrix
K = [1.5 -1 0 0 0 0; -1 3 -1 0 0 0; 0 -1 3 -1 0 0; 0 0 -1 3 -1 0; 0 0 0 -1 3 -1; 0 0 0
0 -1 3];

% [R] is 6x6 diagonal matrix with the values of r= 1.3333
R = [1.3333 0 0 0 0 0; 0 1.3333 0 0 0 0; 0 0 1.3333 0 0 0; 0 0 0 1.3333 0 0; 0 0 0 0
1.3333 0; 0 0 0 0 0 1.3333];

% [L] is 6x6 matrix with the values of series and mutual inductances
L = [0.4310 0.2392 0.1435 0.0947 0.0612 0.0496; 0.2392 0.4310 0.2392 0.1435 0.0947
0.0612; 0.1435 0.2392 0.4310 0.2392 0.1435 0.0947;
    0.0947 0.1435 0.2392 0.4310 0.2392 0.1435; 0.0612 0.0947 0.1435 0.2392 0.4310
0.2392; 0.0496 0.0612 0.0947 0.1435 0.2392 0.4310] * 1e-03;

% [T] is 6x6 matrix in the following form:
T = [1 0 0 0 0 0; -1 1 0 0 0 0; 0 -1 1 0 0 0; 0 0 -1 1 0 0; 0 0 0 -1 1 0; 0 0 0 0 -1
1];

% Calculation of [Ei], [Ii], [Ie]
Ei = -1*inv(K)*T;

Ii = -1*inv(L)*R;

Ie = inv(L)*T';

% Compose A matrix
FirstRow = cat(2, zeros(6,6), Ei);
SecondRow = cat(2, Ie, Ii);

A = cat(1, FirstRow, SecondRow);
```

Appendix D. Matlab Code for case of Axial Displacement

Matlab Code for case of Axial Displacement

```
% command returns a state-space model representing the continuous-time
% state-space model of the primary electrical circuit

K = power_analyze('HealthyWinding', 'ss');

% command returns a state-space model representing the continuous-time
% state-space models of (Shunt capacitance Cg is constant)
% Case 1 - where space factor = 3 (change in Cs = 0.1111)
% Case 2 - where space factor = 7 (change in Cs = 0.0204)
% Case 3 - where space factor = 12 (change in Cs = 0.0069)

Z1 = power_analyze('CsChange1', 'ss');
Z2 = power_analyze('CsChange2', 'ss');
Z3 = power_analyze('CsChange3', 'ss');

% Defines range frequencies for analysis
options = bodeoptions;
options.FreqUnits = 'kHz';
options.FreqScale = 'linear';
options.Xlim = {[0, 1000]};
options.YLim = {[0, 130], [-100, 100]};
options.Grid ='on';

bode(Z1, Z2, Z3, options);
childrenHnd =get(gcf, 'Children');
% select magnitude plot
axes(childrenHnd(3))
title('Frequency Response - Axial Displacement');
leg = legend('space factor = 3', 'space factor = 7', 'space factor = 12');
```

Appendix E. Matlab Code for case of Radial Deformation

Matlab Code for case of Radial Deformation

```
% Radial Displacement

% command returns a state-space model representing the continuous-time
% state-space model of the primary electrical circuit

K = power_analyze('HealthyWinding', 'ss');

% command returns a state-space model representing the continuous-time
% state-space models of (Series capacitance Cs is constant)
% Case 1 - where space factor = 3 (change in Cg = 9)
% Case 2 - where space factor = 7 (change in Cg = 49)
% Case 3 - where space factor = 12 (change in Cg = 144)

Q1 = power_analyze('CgChange1', 'ss');
Q2 = power_analyze('CgChange2', 'ss');
Q3 = power_analyze('CgChange3', 'ss');

% Defines range frequencies for analysis
options = bodeoptions;
options.FreqUnits = 'kHz';
options.FreqScale = 'linear';
options.Xlim = {[0, 250]};
options.YLim = {[0, 100], [-100, 100]};
options.Grid ='on';

bode(Q1, Q2, Q3, options);
childrenHnd =get(gcf, 'Children');
% select magnitude plot
axes(childrenHnd(3))
title('Frequency Response - Radial Deformation');
leg = legend('space factor = 3', 'space factor = 7', 'space factor = 12');
```

Appendix F. Matlab Code for Case A1 (TF, poles, zeros)

```
% command returns a state-space model representing the continuous-time
% state-space model of the primary electrical circuit

Or = power_analyze('Original', 'ss');

% Case A1 - change in Cg1 from 0.467 to 0.65
ZA1 = power_analyze('CaseA1', 'ss');

% Convert State Space to Transfer Function
[A, B, C, D] = power_analyze('CaseA1');
[num, den] = ss2tf(A,B,C,D,1);
TFA1 = tf(num, den);
zpk(TFA1);

% Getting poles and zeros
pole(TFA1);
zero(TFA1);

% Defines range frequencies for analysis
options = bodeoptions;
options.FreqUnits = 'kHz';
options.FreqScale = 'linear';
options.Xlim = {[0, 600]};
options.YLim = {[0, 130], [-100, 100]};
options.Grid ='on';

bode(Or, ZA1, options);
childrenHnd =get(gcf, 'Children');
% select magnitude plot
axes(childrenHnd(3))
title('Frequency Response - Case A1');
```